An Evaluation of Statistical Downscaling Methods in Central Canada for Climate Change Impact Studies

by

Kristina Adrienne Koenig

A Thesis submitted to the Faculty of Graduate Studies of

The University of Manitoba

in partial fulfilment of the requirements of the degree of

Master of Science

Department of Civil Engineering

University of Manitoba

Winnipeg

An Evaluation of Statistical Downscaling Methods in Central Canada for Climate Change Impact Studies

BY

Kristina Adrienne Koenig

A Thesis/Practicum submitted to the Faculty of Graduate Studies of The University of Manitoba in partial fulfillment of the requirement of the degree

Of

MASTER OF SCIENCE

Abstract

This study tested two popular statistical downscaling models, the Long Ashton Research Station Weather Generator (LARS-WG) and the Statistical DownScaling Model (SDSM), for their ability to simulate daily time series of local precipitation and temperature for sites in central Canada. The two models were specifically evaluated for their ability to accurately reproduce observed local daily precipitation and temperature means and variability (extremes). Results of the evaluation using available data in central Canada indicated that both models were able to describe the basic statistical properties of daily minimum and maximum temperatures at local sites. However, SDSM could not simulate the extremes of precipitation well while LARS-WG demonstrated more skill at simulating the means and extremes of precipitation. The skill of SDSM with predictors from CGCM3 was degraded relative to NCEP predictors suggesting the presence of bias in the CGCM3 predictors. A trend analysis in the study area showed an increasing temperature trend. Future downscaled climate change scenarios using SDSM and LARS-WG for the 2050s and 2090s were generated.

Acknowledgements

I would like to express my gratitude to my supervisor, Dr. Peter Rasmussen, whose expertise, understanding and patience added considerably to my graduate experience. I would also like to thank the other members of my examining committee Dr. Shawn Clark and Mr. Bill Girling for taking time out of their schedules to serve on my examining committee.

A very special thanks goes to Dr. Elaine Barrow, Dr. Robert Wilby, and Ms. Suzan Lapp for providing the methodologies to derive the predictor variables used in this study and Lucie Vincent and Eva Mekis for providing the homogenized data. I must also acknowledge Dr. Phillipe Gachon, Dr. Robert Wilby, Dr. Roger Nelson and Mr. Efrem Teklemariam for their expertise advice and technical support throughout this thesis. I want to thank all my friends and colleagues for all their help, support, and valuable hints throughout my graduate experience.

Most importantly, I would like to thank my family for the support they provided me through my entire life and in particular must acknowledge my dad (Karl Koenig), my mom (Irene Koenig) and my brother (James Koenig). Without their constant encouragement, support, and assistance, I would not have finished this thesis. They have always supported and encouraged me to do my best in all matters of life. To them I dedicate this thesis.

In conclusion, I recognize that this research would not have been possible without the financial assistance of Manitoba Hydro, the Natural Science and Engineering Research Council of Canada, and the Prairie Adaptation Research Collaborative.

To my family

Table of Contents

List of Figures

List of Tables

List of Abbreviations

ASDM	Automated Statistical Downscaling Model
AOGCM	Atmosphere-Ocean General Circulation Model
AGCM	Atmospheric General Circulation Model
CCCma	Canadian Center for Climate Modeling and Analysis
CDD	Consecutive Dry Days
CGCM3	Third Generation Canadian Global Climate Model
ClimGen	Climatic Data Generator
DTR	Diurnal Temperature Range
GCM	Global Climate Model
IPCC	Intergovernmental Panel on Climate Change
IQR	Inter-quartile-range
LARS-WG	Long Ashton Research Station Weather Generator
NCEP	National Center for Environmental Prediction
OGCM	Ocean General Circulation Model
PDF	Probability Density Function
RCM	Regional Climate Model
SRES	Special Report on Emission Scenarios
SDSM	Statistical DownScaling Model
SDSM-NCEP	Statistical DownScaling Model with NCEP predictors
SDSM-CGCM3	Statistical DownScaling Model with CGCM3 predictors
Tmax	Maximum Temperature
Tmin	Minimum Temperature
Q-Q plot	Quantile-Quantile plot
WGEN	Weather Generator

Chapter 1

Introduction

1.1 General

Within the scientific community there is a strong agreement that climate change is taking place. The summary of the Fourth Assessment Report (AR4) released in February of 2007 by the Intergovernmental Panel on Climate Change (IPCC) confirmed that the "warming of the climate system is unequivocal, as is now evident from observations of increases in global average air and ocean temperatures, widespread melting of snow and ice, and rising global average sea level" (IPCC 2007, pg 5). The IPCC (2007, pg 5) further stated that the 100 year linear trend (1906-2005) has increased from their previous assessment (1906-2000) of +0.6°C to +0.74°C and that a global warming of about +0.2°C per decade is anticipated over the next twenty years with future temperature increases beyond this period dependent upon the future global greenhouse gas emission patterns (IPCC 2007, pg 12). These temperature changes will likely impact the world's resources, through an increase in precipitation and evaporation. Resource managers must therefore develop a comprehensive understanding of the scope, magnitude, and timing of these impacts by examining climate scenarios to determine the best management techniques to address future climate change.

1.1.1 Weather, Climate, and Climate Change

Weather is defined as the day to day variations in temperature, rainfall, snowfall, wind, clouds, and other weather elements. It is the fluctuating state of the atmosphere around us and is the result of developing and decaying weather systems (Baede et al. 2001, pg 87).

Climate is the average weather in terms of its mean and variability in a specific area over a specified time span. Climate will vary depending on the latitude, presence or absence of mountains, distance to the sea and other geographical factors, as well as on a time scale from season to season, or decade to decade. Atmospheric circulation patterns and their interactions with large scale ocean currents and land, including factors which influence the radiative balance (i.e. greenhouse gases), determine climate and make up the "climate system". Any changes to the climate system, either natural or anthropogenic, can have an influence on the way it functions. Climate change is therefore defined as variations in the mean state or variability of the climate which persist for decades or longer (Baede et al. 2001, pg 87).

1.1.2 The Greenhouse Effect

Naturally, in this 'climate system' the earth releases back into space as much energy as it receives from the sun in a self-balancing system. The atmosphere generally lets visible light through without absorbing much of it. However, greenhouse gases (which consist of only about 1 percent of the earth's atmosphere), absorb infrared radiation. It is these

greenhouse gases (i.e. water vapor, carbon dioxide, methane, nitrous oxide, ozone and various chlorine, fluorine, and bromine-containing molecules) which absorb more outgoing infrared radiation and retain it longer before eventually radiating it back into space. The absorption of infrared radiation by greenhouse gases in the atmosphere results in the temperature of the lower atmosphere becoming warmer than it would be if it did not contain them. This is what is called the 'greenhouse effect' and it is an entirely natural process. However, various human activities are increasing the atmospheric concentrations of these greenhouse gases through fossil fuel combustion and other activities and as a result are influencing the earth's climate (Baede et al. 2001, pg 89-94).

1.1.3 Human Influences on the Climate System

Scientists are now confident that the current increase in the average global temperature is very likely (> 90% probability) due to the increase in anthropogenic greenhouse gas concentrations which are affecting the radiative balance of the climate system (IPCC 2007, pg 10). Since the mid 20th century, the earth has experienced a continual rise in the average global temperature and that increase in temperature is classified as the current climate change. It is understood that the earth's climate has change in the past; however, the cause of the current climate change differs from the past. The current change in climate over the past fifty years is attributed to anthropogenic activities, while changes previous to the last fifty years were due to natural origins (IPCC 2007, pg 12).

1.1.4 Future Projections of Climate

In order for policymakers and resource managers to understand the magnitude and timing of these climate change impacts and their effect on local and regional resources, they must be able to study climate scenarios of key climate variables for future time periods. There are three main classes of climate change scenarios which are used to develop climate scenarios: synthetic scenarios, analogue scenarios, and scenarios based on outputs from general circulation models also known as global climate models (GCMs) (Carter et al. 2007). Of these three classes of climate change scenarios, those based on GCM outputs are currently the most reliable for deriving climate change scenarios and estimating climate change impacts for the future. The public often questions the ability of scientists to project climate fifty years into the future when weather cannot be accurately predicted two weeks ahead. However, projecting changes in long term weather (i.e. climate) due to atmospheric composition changes or other factors is very different and much more manageable than predicting weather which has a chaotic behavior (Le Treut et al. 2007, pg 96).

1.2 Problem Statement

Climate change impact studies at local sites usually require daily time series of surface weather variables, such as precipitation and temperature, for future climate scenarios. GCMs have recently been widely used to simulate the past, present, and future climate. GCMs are numerical models that represent the large-scale physical processes of the

earth-atmosphere-ocean system. They are able to project future climate under a range of scenarios including those forced by greenhouse gases and aerosols. They are, however, restricted in their usefulness for local impact studies due to their inability to resolve important sub-grid scale features such as topography and mesoscale atmospheric processes due to their coarse spatial resolution (von Storch et al. 1993; Wilby and Dawson 2004; Wilby and Wigley 2000). Specifically, hydro-meteorological outputs from GCMs are unreliable for individual grid points as their spatial resolution is too coarse to resolve important catchment-scale processes (Hostetler 2005; Xu 1999).

In order to bridge the gap and scale down the information between the coarse GCM resolution and the sub-grid process required by impact modelers, downscaling techniques have been developed. There are two main types of downscaling techniques: dynamical downscaling and statistical downscaling (Dibike and Coulibaly 2007; Wilby et al. 2000).

- Dynamical downscaling techniques use GCM information as the boundary conditions to drive a regional climate model (RCM) which is able to simulate finer-scale physical processes, typically at a grid resolution of 20-50 km (Giorgi and Mearns 1999; Mearns et al. 2003; Wilby and Dawson 2004; Xu 1999).
- Statistical downscaling techniques involve establishing empirical relations between features reliably simulated by the GCM (such as upper atmospheric circulation variables) and surface predictands (such as temperature) (Wilby et al. 1999).

To date there have been several downscaling techniques proposed in the scientific literature, each having its own advantages and shortcomings. It is not clear which downscaling technique provides the most reliable simulation of climatic variables since there are factors such as the topography of a region which can influence the performance of a downscaling model. Therefore, a rigorous evaluation of the various downscaling techniques must be performed to identify the most robust method(s) for a given location.

1.3 Research Objectives

The main objective of this study is to test two popular statistical downscaling models, the Statistical DownScaling Model (SDSM) and the Long Ashton Research Station Weather Generator (LARS-WG), for their ability to simulate daily time series of local precipitation and temperature at meteorological stations located in central Canada. Six stations have been selected for this research: two in northern Manitoba (Thompson and The Pas), two in southern Manitoba (Winnipeg and Brandon), and two in northwestern Ontario (Kenora and Sioux Lookout). The evaluation of these models will consist of examining their ability to simulate means and extremes indices.

The other objectives of this study are to:

- Evaluate historical trends in temperature and precipitation.
- Generate missing solar radiation data.
- Generate future downscaled climate change scenarios using SDSM and LARS-WG with the Third Generation Canadian Global Climate Model (T47)

using three future emission scenarios for two future decadal periods.

1.4 Thesis Organization

Chapter 2 presents background information relevant to this research. It introduces common terminology used in climate impact studies as well as provides a general introduction to downscaling, highlighting the best practices to statistical downscaling. Detailed descriptions of SDSM and LARS-WG along with an overview of the various studies where these models have been tested and applied are also presented.

Chapter 3 provides a description of the data sources and study area. It describes the current climate at the meteorological stations in the study area.

Chapter 4 describes the evaluation of the solar radiation model, Climatic Data Generator. This model was utilized to simulate historical solar radiation at the meteorological stations where solar radiation was not available.

Chapter 5 summarizes the methodology used to determine historical climate trends, select predictors, evaluate SDSM and LARS-WG, and develop future climate change scenarios.

Chapter 6 provides details regarding historical climate trends, the evaluations of SDSM and LARS-WG, and climate change scenarios at the meteorological stations.

Chapter 7 provides conclusions that were drawn from the research and recommendations for future study.

Chapter 2

Literature Review

2.1 Introduction

This chapter provides a summary of the literature related to the development of climate scenarios for climate impact studies. An overview of GCMs is presented, outlining their deficiencies for use in climate impact studies along with their associated uncertainties. A general overview of downscaling techniques is given along with some best practices recommended by the IPCC for statistical downscaling. This chapter also describes details of the SDSM and LARS-WG models and summarizes the models' application in the literature.

2.2 Construction of Climate Scenarios

A comprehensive analysis of current climate (also referred to as baseline climate), including any changes in variability, must be conducted at the beginning of any climate impact study. This is required to understand the current climate system and the significance of the projected future changes (Barrow and Lee 2000). The average climate over a 30-year period is commonly used to define the baseline climate to smooth out any year-to-year variations. This 30-year period is also intended to capture the inter-annual and short time scale variability in climate that may be relevant in a climate impact study. The period 1961-1990 has been recommended to be used as the baseline climate by the

IPCC (Mearns et al. 2001, pg 749) since it generally has good observed data and it represents the recent climate that many present-day human or natural systems have grown accustomed and adapted to.

There are many terms to describe future climate. To ensure that the terminology in this report is consistent with the scientific literature, the terms recommended by the IPCC will be used throughout this report (Mearns et al. 2001, pg 743):

- Climate projection: A description of the response of the climate system to a scenario of greenhouse gas and aerosol emissions as simulated by a global climate model. Projections alone can rarely provide sufficient information to examine future impacts since the outputs must be manipulated and combined with observed climate to be used in a climate impact study.
- Climate change scenario: This is an interim step towards constructing a climate scenario and should be strictly referred to as the difference between some plausible future and current climate, usually represented by GCMs. In statistical downscaling, a climate change scenario represents the difference between a set of values simulated for future climate and the values simulated for current climate by the statistical downscaling model.
- Climate scenario: Represents a plausible future which is consistent with assumptions of future greenhouse gas emissions and the effects of their composition in the atmosphere. It consists of combining the climate change

scenario with baseline climate observations. This method is commonly used when raw GCM outputs are used in an impact model. In general, when statistical downscaling techniques are employed the baseline climate observations are used in the development of the future climate scenarios and therefore do not require the simulated datasets to be added to the original baseline climate.

As described in Chapter 1, there are several types of climate change scenarios used to develop climate scenarios: synthetic scenarios, analogue scenarios, and scenarios based on outputs from GCMs (details in Carter et al. 2007). Climate change scenarios based on GCM outputs are currently the most credible tool for developing future climate scenarios (Barrow and Lee 2000; Carter et al. 2007). This is because GCMs meet the following criteria established by the IPCC for the development of climate change scenarios (Carter et al. 2007):

- Consistency with global projections: The scenarios should fall within a wide range of climate change projections based on increased atmospheric concentrations of greenhouse gases.
- Physical plausibility: The scenarios should be consistent with the physical laws that govern climate. Changes in one region should be consistent with those in other regions.
- Applicability in impact assessments: The scenarios should describe changes in a

large number of climate variables (spatially and temporally) that allow for climate impact assessments.

- Accessibility: The scenarios should be straightforward to obtain, interpret, and apply.

This study develops climate change scenarios based on GCMs outputs.

2.3 Global Climate Models (GCMs)

Global climate models (GCMs) are numerical models that represent the large-scale physical processes of the earth-atmosphere-ocean system. They have been designed to simulate the past, present, and future climate. GCMs can represent the physical processes in the atmosphere, ocean, land surface, and cryosphere by solving a series of equations based on the conversation of mass, momentum, and energy. They are able to do this in all three spatial directions: a horizontal resolution between 250 and 600 km, a vertical resolution up into the atmosphere of between 10 and 20 layers, and up to 30 layers of depth down into the ocean (Barrow and Lee 2000; Carter et al. 2007).

Currently, the most sophisticated types of GCMs available are the coupled atmosphere-ocean general circulation models (AOGCM). These GCMs consist of an atmospheric general circulation model (AGCM) coupled to an ocean general circulation model (OGCM), along with sea-ice models and models of land surface processes (McAvaney et al. 2001, pg 475). The AGCMs consist of a three-dimensional

Table 2.1: Global climate model descriptions

Model	*Atmosphere Component*	*Ocean Component*
HadCM3, United Kingdom	2.5° lat. X 3.75° long. 19 vertical layers	1.25° lat. X 1.25° long. 20 vertical layers
HadGEM1, United Kingdom	1.25° lat. X 1.875°long. 38 vertical layers	1° lat. X 0.333-1° long. 40 vertical layers
CGCM3, Canada	~3.75° lat. X 3.75° long. 31 vertical layers	~1.85° lat. X 1.85° long. 29 vertical layers
CSIRO Mk3, Australia	~1.875° lat. X 1.875° long. 18 vertical layers	~0.84° lat. X 1.875° long. 31 vertical layers
MICROC3, Japan	~2.8° lat. X 2.8° long. 20 vertical layers	1.4° lat. X 0.56-1.4° long. 43 vertical layers

representation of the atmosphere coupled to the land surface and cryosphere, and the OGCM is a three-dimensional representation of the oceans and sea-ice (Saelthun and Bark 2003). Since AOGCMs are able to model the entire earth-atmosphere-ocean system, they are most suitable for projecting future climate.

There are many modeling centers around the world that have developed GCMs based on their own unique algorithms and grid size. They are documented in the IPCC's Third Assessment Report (Cubasch et al. 2001, pg 538-539). Table 2.1 lists a selection of the GCMs available with their respective resolutions.

Since there are many GCMs available to the climate impact modeling community, researchers have outlined the following criteria to guide the selection of GCMs (Barrow and Lee 2000; Carter et al. 2007; Smith and Hulme 1998):

- Vintage: More recent GCMs are most likely more reliable than those of an early vintage. This is because the most recent knowledge has been incorporated into the processes and feedbacks of these GCMs.

- Resolution: More recent GCMs have spatial resolution much finer than the earlier GCMs. This allows for more spatial details including better defined land and sea boundaries along with more complex topography to be incorporated.

- Validity: It is generally assumed that GCMs which simulate the present-day climate most faithfully will ultimately provide the most reliable representation of future climate. The GCM performance depends critically on the size of the region, the location, and the variables being analyzed. However, even if a GCM simulates present day climate well, it does not necessarily imply that the GCM will produce accurate simulations of climate change (McAvaney et al. 2001, pg 473). For example, a GCM will not provide an accurate simulation of climate change if the model does not contain a good representation of the dominant feedback processes that will be initiated by radiative forcing (Mearns et al. 2001, pg 760).

- Representation of results: It is strongly recommended that more than one GCM be used in any climate change impact study. The selected GCMs will illustrate a range of values for the key climate variables such as precipitation and temperature in the study region. When examining the outputs from various GCMs at a regional level they can display large differences in their estimates of climate variables and therefore it is imperative that the range is captured in any climate impact study.

2.3.1 Emission Scenarios

It is necessary to construct scenarios of greenhouse gas and sulphate aerosol emissions of the next 100 years and beyond to determine how the composition of the atmosphere, and consequently climate, may change in the future. These emissions scenarios require assumptions about how society will evolve into the future. Emissions scenarios are used in GCMs to simulate the evolution of climate over time.

Until recently, most climate modeling centers used the IS92 scenarios, which are detailed in Climate Change 1992: Supplementary Report to the IPCC Scientific Assessment (Houghton et al. 1992). These scenarios consist of six emissions scenarios, IS92 a-f, with IS92e and IS92c resulting in the highest and lowest atmospheric greenhouse gas concentrations respectively. The IS92a scenario became known as the 'business-as-usual' scenario.

Prior to issuing its Third Assessment Report (IPCC 2001), the IPCC commissioned a Special Report on Emissions Scenarios (SRES) (IPCC 2000). The purpose of the SRES was to provide scientists with background information for use in drafting the Third Assessment Report, which was released in 2001. The same scenarios were used in 2007 for the Fourth Assessment Report. The SRES describes four principal, yet different narrative 'storylines' (A1, A2, B1, B2) representing different demographic, social, economic, technological, and environmental developments. Based on these storylines, four 'scenario families' are identified and a total of 40 emissions scenarios were developed.

The associated storylines are as follows (IPCC 2000):

- A1 storyline: The A1 storyline and scenario family looks into the future to a world with a population peaking by 2050 and then declining with rapid economic growth from new and efficient technologies being developed.
- A2 storyline: The A2 storyline and scenario family looks at a mixed world with regional economic development, slow per capita growth, and slow fragmented technological growth.
- B1 storyline: The B1 storyline and scenario family looks at a convergent world with world populations similar to A1, peaking by 2050 and subsequently dropping. However, in this world economic structures are quickly developing in a service and information economy with less emphasis on material goods and more emphasis on clean, efficient resources, and technologies.
- B2 storyline: The B2 storyline and scenario family is a world which stresses home-made solutions to economic, social, and environmental sustainability. This world has a steady population growth lower than A2 with median economic development, and a slower much more diverse technological development than scenario B1 and A1.

Of the forty SRES scenarios available, two have emerged to have particular significance by the scientific community. These are the A2 scenario referred to as the "business as usual" or "worse case" scenario, and the B2 scenario, referred to as the "best

guess" or "most likely" scenario (Källén et al. 2001).

2.3.2 Uncertainties Associated with GCMs

When simulating climate change scenarios using GCMs there are many uncertainties to be considered. There is a lack of understanding of certain scientific principles and processes which govern the climate; therefore, incorporating these physical processes into the simulations with computer based tools is difficult. Furthermore, there are uncertainties in the projections of future climate which rely on emission scenarios involving assumptions based on population growth, economic growth, and energy use.

The IPCC-TGCIA (1999) has identified the following main sources of uncertainties involved when applying scenarios from GCMs:

- Uncertainties in future greenhouse gas and aerosols emissions: There is a range of responses in global mean temperature associated with the various emission scenarios.
- Uncertainties in global climate sensitivity: Each GCM simulates the physical processes and feedback defining climate in different ways. Different models produce different estimates of global warming for the same emission scenario.
- Uncertainties in regional climate changes: The output from different GCMs at the regional level indicates different response for the same mean global warming.

2.3.3 Mismatches Between GCMs ability and Climate Impact Modelers Needs

It is apparent that most GCMs are reasonably accurate at representing the climate at the continental and hemispheric spatial scales. However, they are inherently weak in representing local sub-grid scale features and dynamics. This makes them unsuitable to many impact modelers, particularly hydrologists interested in regional-scale hydrological variability (Dibike and Coulibaly 2007; Mearns et al. 2003) .

According to Xu (1999) there are three main mismatches between GCMs and the needs of hydrological impact modelers:

- The spatial scale mismatch between GCM resolution and hydrological needs: Hydrologic models typically are based on small sub-basin scale. GCMs prevent explicit modeling of local geographic factors such as basin topography, land-water distribution, and vegetation type.
- The vertical level mismatch between GCM resolution and hydrological needs: GCMs are more adept in simulating the free troposphere climate than the surface climate since the free troposphere is more spatially and temporally homogenous than the earth's surface. However, problems arise because hydrologic modelers require accurate representation of the earth's surface variables, which GCMs are not able to simulate well.
- The mismatch between GCM accuracy and the hydrological importance of the variables: The GCM outputs such as wind, temperature, and air pressure fields

can be reasonably accurate since the GCMs were designed to simulate average large-scale atmospheric circulation. On the other hand, variables such as clouds, precipitation, runoff, soil moisture, and evapotranspiration are not well represented by GCMs (Loaiciga et al. 1996). Basically, the GCM simulation accuracy decreases from climate variables to hydrological variables while the hydrological importance increases along the same direction. Precipitation, which is a hydrological variable of great importance to hydrological modelers, is not well represented by GCMs because many significant precipitation events such as thunderstorms happen on a much smaller spatial scale than the GCM grid size.

2.4 Downscaling Techniques

Several downscaling techniques have been developed to counter the deficiency in GCMs by "downscaling" the meteorological variables to a scale which is useful for climate impact studies (i.e. Hewitson and Crane 1996; Murphy 1998; Wilby and Wigley 2000; Wilby et al. 1998). There are two main branches of downscaling: dynamical downscaling and statistical downscaling (Dibike and Coulibaly 2007).

2.4.1 Dynamical Downscaling

Dynamical downscaling or regional climate modeling uses the concept of limited area modeling at a higher resolution to obtain regional details that the GCM can not achieve due to its coarse scale in the area of interest. The basic concept in this type of

downscaling is to let the GCM provide the lateral and initial boundary conditions for a regional climate model (RCM). The RCM allows for a more accurate description of the regional topography, lakes, and coastlines since the grid resolution is much higher, typically between 25-50 km (Jones et al. 1995).

RCM simulation can be computationally demanding depending on the size of the domain being modeled and therefore may be limited in the length of the experiment. Also, since RCMs simulate on a scale between 25 km to 50 km, there may be times when this scale is still larger than what is required by impact modelers and therefore direct application is not possible. In such cases, statistical downscaling techniques may be required to downscale the RCM to a more suitable scale (i.e. station level). A more problematic consideration in the use of RCMs is that their results are strongly influenced by the selection of the GCM and any deficiencies in the GCM can propagate back to the RCM.

2.4.2 Statistical Downscaling

In the literature statistical downscaling techniques are grouped into three categories (Wilby and Dawson 2004):

1) Transfer function models or regression-based models: Transfer function methods, also referred to as regression based methods, rely on a direct quantitative relationship between variables containing the large scale information (predictors) and the local scale climate variables (predictands) through a regression function

(Dibike and Coulibaly 2007; Wigley et al. 1990). This method uses statistically based models to determine the relationship between the predictor and predictands for current climate and then applies similar predictors from GCM simulations in the statistical models to project future climate (Wilby et al. 2004). There are many types of mathematical transfer functions that have been used successfully in statistical downscaling including multiple regression, canonical correlation analysis, and artificial neural networks (Girogi et al. 2001, pg 617; Wilby et al. 2004). When applying the transfer function methods there are some implicit assumptions (Girogi et al. 2001, pg 616; Wilby et al. 2004; Wilby and Wigley 2000):

- The predictors fully represent the climate change signal.
- The predictors are variables of relevance and are realistically modeled by the GCM.
- The relationship is valid also under an altered climate condition.
- The predictors are physically linked to the appropriate local predictand.

The main advantage of transfer function methods is that they are relatively straightforward to apply and are computationally less demanding in comparison to other downscaling methods. However, they are limited in their application to areas where accurate predictor-predictand relationships can be found (Wilby et al. 2004; Wilby and Dawson 2004).

2) Stochastic weather generators: Stochastic weather generators can be described as statistical models of observed sequences of weather variables or complex random number generators in which the outputs represent daily or sub-daily weather data at a particular site of interest (Wilks and Wilby 1999). The output of the weather generator is usually in the form of precipitation occurrence and intensity, maximum and minimum temperature, and solar radiation. Generally, the parameters in the weather generators are conditioned on relationships between large-scale parameters sets and local-scale parameters (Wilks and Wilby 1999), or by perturbing the parameters based on GCM simulated changes in the statistics of some climate variables (Semenov and Barrow 1997). The main advantage of stochastic weather generators is that they can reproduce many observed climate statistics. A disadvantage is that the adjustment of the parameters of the future climate are somewhat subjective (Wilby et al. 2004).

3) Synoptic weather typing: Synoptic weather typing relates weather classes to regional or local climate variations by grouping days according to their synoptic similarity into a finite number of discrete weather types or states (Girogi et al. 2001, pg 618; Wilby et al. 2004). In order to estimate a change in climate, the changes in the frequency of weather classes, derived by weighing the local climate states with their relative frequencies of weather classes from current to future climate, are compared (Girogi et al. 2001, pg 618). Weather typing methods are versatile and therefore can be applied to a variety of different surface

climates. However, a critical weakness is that they assume that the characteristics of the weather classes do not change in future climate (Wilby et al. 2004; Wilby and Dawson 2004).

Many studies which apply statistical downscaling focus on daily maximum temperature and minimum temperature, as well as precipitation at a single site since it is the most important input for many impact models (Wilby et al. 2004). When statistical downscaling techniques are employed, a sufficient amount of observed data is required in the study area to calibrate the models.

The theoretical weaknesses of statistical downscaling is that it is not verifiable (which also applies to the physical parameterization of regional climate models) and that it assumes that the statistical relationship developed for the present day climate also holds under the future climate (Wilby et al. 2004). However, despite these weaknesses statistical downscaling has a number of advantages including being computationally inexpensive which allows the methods to be applied using a variety of GCMs (Wilby et al. 2004).

2.5 Good Practise to Statistical Downscaling

In order to gain confidence in statistical downscaling climate scenarios for climate impact studies and to ensure that climate impact modellers adhere to best practises, the IPCC established a "Guideline for Use of Climate Scenarios Developed from Statistical Downscaling Methods" (Wilby et al. 2004). The following outlines some important

practises recommended by these guidelines to be followed when applying statistical downscaling:

- Specify appropriate model type: There are a range of statistical downscaling techniques available to the climate impact modeling community. The skill of the chosen technique ultimately depends on the chosen application and study region. The choice of the downscaling model will also reflect the availability of computer models, the availability of data, and the time step of output required.

- Select appropriate predictor variables: The downscaled climate scenario is ultimately governed by the choice of predictor variable, thereby making the selection of predictors one the most important steps in many statistical downscaling techniques. However, there are only a few studies which have analysed the significance of different predictor variables. Expert judgement, local knowledge, and sensible combinations of predictors should all be taken into consideration in the selection process. Some key ideas when selecting predictors are as follows:

    - In the future, atmospheric moisture which currently has some control over present day precipitation will have a greater significance (Hewitson 1999). When downscaling precipitation, the inclusion of atmospheric moisture is imperative as it may be critical in capturing the climate change signal and has an impact on both the sign and magnitude of precipitation change in the future (Hewitson 1999; Wilby et al. 2004).

- In the future, changes in the radiative properties of the atmosphere may dominate over circulation changes that currently control our present-day surface temperature (Schubert 1998). When downscaling temperature, both circulation fields and surface temperature should be analyzed, since utilizing predictors based solely on atmospheric circulation could result in potential cooling trends (Huth 1999).
- When selecting predictors, there is a risk of discarding predictor variables which have a low explanatory power for present climate, but which are critical for evaluating climate change. Therefore judgment should be used when selecting predictors. Predictors which are only pertinent to present day climate should not be used exclusively.

- Assess the value of downscaling: After a series of climate change scenarios have been developed, the value gained from using a statistical downscaling technique beyond the use of raw GCM output should be evaluated. This is accomplished by testing the downscaled outputs and the raw GCM outputs relative to observed climatology under present climate conditions.

2.6 Statistical Downscaling Software Packages

At the time of this study, there were four statistical downscaling software packages developed or in the processes of being developed. Each of these software packages is described in Table 2.2 by the type of statistical downscaling technique employed.

Table 2.2: Statistical downscaling software packages

Software Package	*Available to public?*	*Transfer Function*	*Weather Generator*	*Weather Typing*
Statistical DownScaling Model (SDSM)	yes	yes	yes	no
Long Ashton Research Station Weather Generator (LARS-WG)	yes	no	yes	no
Weather Generator (WGEN)	yes	no	yes	no
Automated Statistical Downscaling Model (ASDM)	no	yes	yes	no

The Weather Generator (WGEN) is similar to LARS-WG. However, due to limitations of WGEN (described in Section 2.7), LARS-WG was selected for evaluation rather than WGEN. SDSM is a hybrid of a regression based method and a weather generator; therefore was also selected to be evaluated. The Automated Statistical Downscaling Model (ASDM) was in the development stage at the time of study and therefore was not available to be tested.

2.7 Long Ashton Research Station Weather Generator (LARS-WG)

The Long Ashton Research Station Weather Generator (LARS-WG) (Version 3.0) is a stochastic weather generator used to simulate daily weather variables (maximum temperature, minimum temperature, precipitation and solar radiation) at a single site under both current and future climate (Semenov and Barrow 2002).

The simulation of daily weather variables from stochastic weather generators generally involves one of the following methods: Richardson-type approach (Richardson

1981) or serial approach (Rascko et al. 1991). Both of these methods employ the same fundamental steps. The first step involves modeling the daily precipitation occurrence and the second involves modeling additional variables such as maximum temperature, minimum temperature, precipitation amount, and solar radiation.

The Richardson-type approach uses a Markov Chain model to describe the occurrence of wet and dry days, and then models the amount of precipitation falling on the wet days using an estimated distribution of precipitation depth. The remaining variables are then modeled based on the wet or dry status of each day and their correlations to each other. One of the main criticisms of this approach is its limited memory of rare events and its inability to describe adequately the length of dry and wet series (Rascko et al. 1991).

LARS-WG uses the "serial approach" to overcome the limitations of the Markov Chain Model. This involves, as a first step, modeling the length of the dry and wet series using semi-empirical distributions (Semenov et al. 1998). Then the amount of precipitation, daily solar radiation, maximum temperature, and minimum temperature are modeled conditioned on the precipitation status.

Precipitation occurrence is modeled as alternate wet and dry series where the length of each series is chosen randomly from the wet or dry semi-empirical distribution for the month at which the series starts. The daily means and standard deviation of both minimum and maximum temperatures are conditioned on the wet or dry status of the day and are considered as stochastic processes. In order to account for the seasonal cycles in

the mean and standard deviation of temperature, a Fourier series is used to smooth the data with the residuals approximated by a normal distribution. Solar radiation is modeled independently of temperature, with separate semi-empirical distributions used to describe solar radiation on wet and dry days.

One of the important features of LARS-WG is that it uses all the observed records to generate the semi-empirical distributions, making it more flexible than parametric distributions. Semenov et al. (1998) conducted a study to compare two weather generators (WGEN and LARS-WG) for sites in Europe, USA, and Asia. They found that because LARS-WG uses semi-empirical distributions, it was able to simulate climate data with statistics much closer to the observed data at a variety of sites making it more flexible than WGEN which is based on fixed distributions.

Details pertaining to the procedures in LARS-WG to generate time-series of daily precipitation, temperature, and solar radiation are presented in Semenov and Barrow (2002). The general process is as follows:

- Model calibration: Observed weather data for a specific meteorological site is analyzed to create a parameter file (.wg). This parameter file is required to generate synthetic weather data. Table 2.3 outlines the parameters stored and used to develop the distributions.

  Generation of synthetic weather data: The parameter file derived during the model calibration process is used to generate synthetic weather data having the

Table 2.3: LARS-WG parameters

Parameter	*Description*
Series	Monthly histogram intervals and frequency of events in these intervals for wet and dry series length.
Precipitation	Histogram intervals and frequency of events in these intervals for precipitation amount by month.
Wet Min	Fourier coefficients for the means and standard deviation of minimum temperatures on wet days.
Wet Max	Fourier coefficients for the means and standard deviation of maximum temperatures on wet days.
Dry Min	Fourier coefficients for the means and standard deviation of minimum temperatures on dry days.
Dry Max	Fourier coefficients for the means and standard deviation of maximum temperatures on dry days.
Auto Min	Average autocorrelation value for minimum temperature.
Auto Max	Average autocorrelation value for maximum temperature.
Auto Rad	Average autocorrelation value for solar radiation.
Wet Rad	Monthly histogram interval values and frequency of events in each interval for solar radiation amounts on wet days.
Dry Rad	Monthly histogram interval values and frequency of events in each interval for solar radiation amounts on dry days.

same statistical characteristics as the original observed data.

- Climate scenarios: Future climate scenarios are derived by perturbing the parameters using a scenario file. This scenario file is based on GCM simulated changes in monthly precipitation, length of wet series, length of dry series, minimum temperature, maximum temperature, standard deviation of temperature, and mean solar radiation.

2.8 Statistical DownScaling Model (SDSM)

The Statistical DownScaling Model (SDSM) (Version 3.1) is a hybrid between a transfer function/regression based method and a stochastic weather generator since it uses multiple linear regression techniques to derive relationships between large-scale atmospheric variables (predictors) and local-scale variables (predictands) and then adjusts the variance of the downscaled data using a stochastic process (Wilby et al. 2002). The variables modeled by SDSM include maximum temperature, minimum temperature and precipitation.

Details pertaining to the model structure and processes can be found in Wilby and Dawson (2004). Generally, temperature and precipitation are modeled as follows:

- Temperature: Daily maximum ($Tmax_i$) and minimum ($Tmin_i$) temperatures for a given day are modeled using the following regression equations (Wilby et al 1999):

$$Tmax_i = \delta_o + \delta_T Tmax_{i-1} + \delta_1 P_1 + \cdots + \delta_k P_k + \xi_i \qquad \textbf{Eq. 2.1}$$

$$Tmin_i = \gamma_o + \gamma_T Tmin_{i-1} + \gamma_1 P_1 + \cdots + \delta_k P_k + \zeta_i \qquad \textbf{Eq. 2.2}$$

where δ and γ are parameters estimated by linear least squares regression, ξ and ζ are random or modeling errors and P_i is a predictor variable.

- Precipitation: Precipitation is downscaled with SDSM following a conditional process consisting of two different steps (Wilby et al. 1999). The first step involves developing a linear regression between large scale predictors and the

probability of precipitation occurrence. Daily precipitation occurrence O_i is modeled using the following equation (Wilby et al. 1999):

$$O_i = \alpha_o + \alpha_{i-1} O_{i-1} + \alpha_1 P_1 + \cdots + \alpha_k P_k \qquad \textbf{Eq. 2.3}$$

where the parameters α_i are estimated using linear least squares regression and P_i is a predictor variable. Then a stochastic process is used to determine whether the day is wet or dry using a uniformly distributed random number r $(0 \le r \le 1)$. There is an occurrence only if this number is less than or equal to the simulated precipitation occurrence probability ($r \le O_i$).

Assuming that precipitation occurs, the second step involves developing another linear regression with large-scale predictors to specify the daily precipitation amounts (R_i). The following regression model is used since the precipitation amounts are always greater than zero (Wilby et al. 1999):

$$R_i = \exp(\beta_o + \beta_1 P_1 + \cdots \beta_k P_k + \varepsilon_i) \qquad \textbf{Eq. 2.4}$$

where the β_i's are parameters estimated using linear least squares regression, ε_i is random or modeling error and P_i is a predictor variable.

A detailed user guide for SDSM is provided in Wilby and Dawson (2004). The general method is as follows (Figure 2.1):

- Data transformation: Transform predictands and/or predictors prior to model calibration.

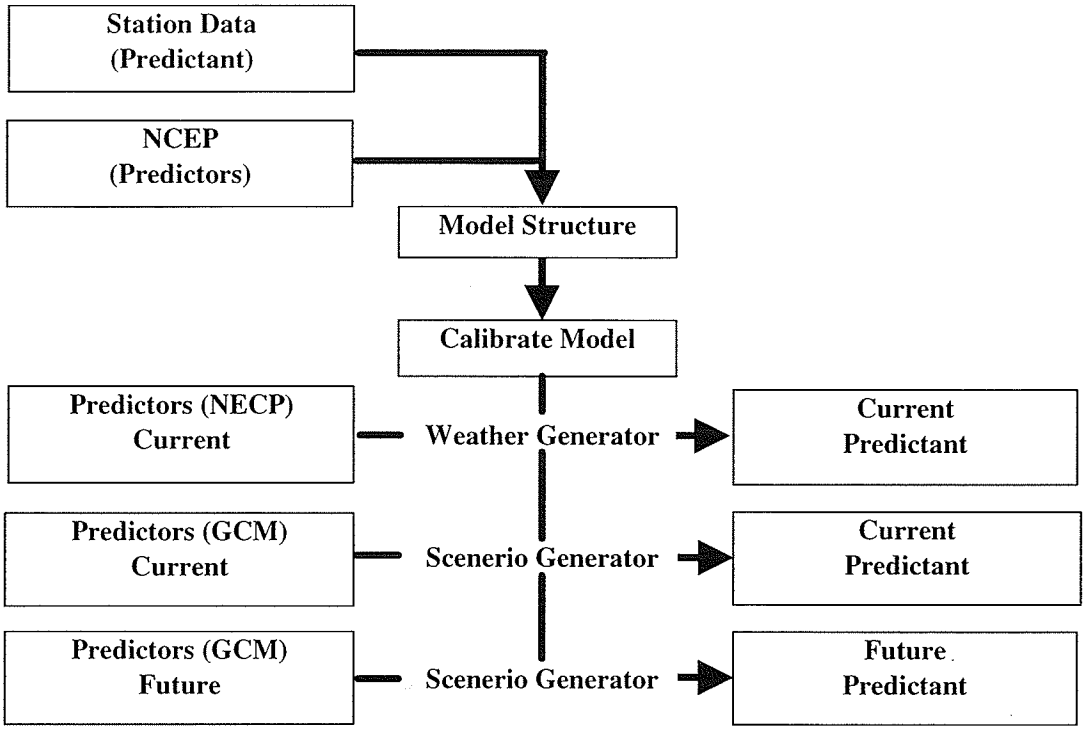

Figure 2.1: SDSM process

- Screening of predictor variables: Select appropriate downscaling predictor variables by identifying empirical relationships between predictors and predictands.
- Model calibration: With a selected predictand and a set of selected predictors the parameters of the multiple linear regression equations are determined.
- Weather generation: Generate an ensemble of synthetic daily weather series given observed gridded (i.e. NCEP predictors) atmospheric predictor variables. This allows the calibrated model to be verified with an independent data set and current climate to be simulated.

- Scenario generation: Generate an ensemble of synthetic daily weather series given GCM supplied atmospheric predictor variables for either current or future climate.

2.9 Studies using SDSM and LARS-WG

SDSM and LARS-WG have been applied to a host of geographical environments including Europe, South Asia, and North America, but with limited application in Canada (Hassan et al. 1998; Haylock et al. 2006; Wilby et al. 1999). These models have also been applied to hydrological and environmental assessment studies (Wilby et al. 2002). With respect to environmental assessments studies, in a research project supported by the Canadian Environmental Assessment Agency, Barrow and Lee (2000) recommended that SDSM and LARS-WG be used for the downscaling of GCMs in the Canadian Environmental Assessment process to derive finer resolution information to assess the impacts of future climate on a project.

SDSM and LARS-WG have not yet been rigorously evaluated over the range of climatic conditions in Canada. Existing studies have focused mainly on areas in eastern Canada. For example, Gachon et al. (2005) compared these models on their ability to downscale extreme indices over regions in eastern Canada. They found that SDSM performed better for temperature than precipitation. Both models were able to capture the precipitation occurrence better than wet day amounts and/or extremes. They also found that LARS-WG precipitation and temperature variability and persistence tended to

be overestimated. In the same study area of eastern Canada, Hessami et al. (2008) found that SDSM shows strength in the simulation of temperature, but had less success for precipitation. Nguyen et al. (2006) evaluated SDSM and LARS-WG for their ability to generate precipitation and temperature extremes in the Greater Montreal region. They found that both models were able to accurately describe the basic statistical properties of daily maximum and minimum temperature at the sites with neither of the models able to simulate well the statistical properties of the daily precipitation process. However, LARS-WG was able to produce statistics of daily precipitation closer to the observed than SDSM.

A study to evaluate SDSM in a highly heterogeneous coastline area of northern Canada was undertaken by Dibike et al. (2007). Their study concluded that the models were able to represent local climate conditions when supplied with accurate GCM predictors. In the Saguenay watershed in Northern Quebec, Mohammad et al. (2006) demonstrated the effects of using GCM predictors from two different generations of the same GCM (CGCM1 and CGCM2) and found that there was a significant variation in estimates of means and variances on a month by month basis, emphasizing the need for accurate predictors from GCMs and that any bias present in the GCM predictors can propagate into the downscaling model. SDSM was also used in a study by Gachon et al. (2005) in the Quebec region that concluded that SDSM provides reasonable downscaled data when using predictors representing the observed current climate (NCEP), but its skill degraded when using GCM predictors. This study again emphasized the need for

accurate predictor variables supplied by the GCMs.

Some studies have used these downscaling models to develop climate scenarios for particular study regions. For example, Dibike and Coulibaly (2007) used both SDSM and LARS-WG to generate possible future scenarios of local meteorological variables. These variables were inputted into a hydrological model to simulate the corresponding streamflow in the Serpent River. Also, Lines and Pancura (2004) used SDSM to develop climate scenarios in Atlantic Canada by examining changes in maximum temperature, minimum temperature, and precipitation. Another impact study used SDSM and LARS-WG to examine the climate change impacts on groundwater recharge in the Gulf Islands south-east of Vancouver Island (Appiah-Adjei 2006). In their study, SDSM and LARS-WG were used to supply local meteorological variables into a groundwater model to simulate groundwater recharge in the region for future time periods.

Chapter 3

Study Area and Data Description

3.1 Study Area

The study region encompasses central Canada (defined as 49°N to 56°N, and 92°W to 101°W). Six meteorological stations were selected with four meteorological stations located in Manitoba and two stations in Northwestern Ontario (Figure 3.1). The latitude and longitude coordinates along with the elevations of the meteorological stations are presented in Table 3.1. These meteorological stations were selected to ensure that a broad range of climatic zones were analyzed. The baseline climate (1961-1990) at these meteorological stations is characterized as follows:

- In the southern Manitoba region (Brandon and Winnipeg), the climate is classified as having a total monthly precipitation ranging from +21 mm during the driest months to +89 mm in the wettest months, and a maximum temperature ranging from −12°C in the winter months to +26°C in the summer months, and a minimum temperature ranging from −25°C in the winter months to +12°C in the summer months (Figure 3.2).
- In the northwestern Ontario region (Kenora and Sioux Lookout) the climate is classified as having a total monthly precipitation ranging from

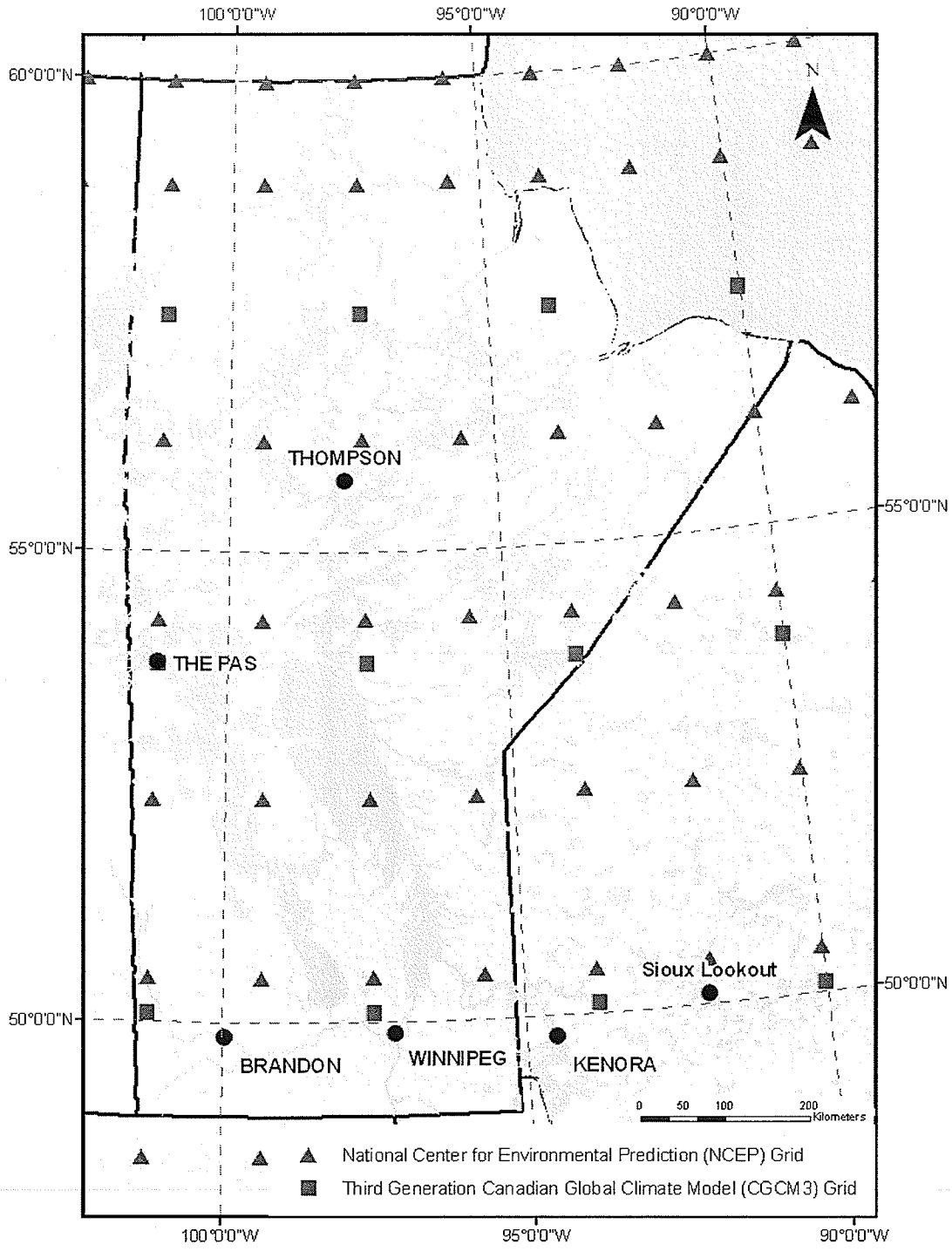

Figure 3.1: Study area

Table 3.1: Meteorological station information

Station Name	*Station #*	*Prov.*	*Lat. (°N)*	*Long. °W (°E)*	*Elev. (m)*
Winnipeg Int'l Airport	5062922	Mb.	49.92	–97.23 (262.77)	239
Brandon Airport	5023222	Mb.	49.87	–99.98 (260.02)	363
Thompson Airport	5052880	Mb.	55.80	–97.87 (262.13)	222
The Pas Airport	5052880	Mb.	53.97	–101.10 (258.90)	270
Sioux Lookout Airport	6037775	Ont.	50.12	–91.90 (268.10)	390
Kenora Airport	6034075	Ont.	49.78	–94.37 (265.63)	406

+32 mm during the driest months to +106 mm in the wettest months, and a maximum temperature ranging from –14°C in the coldest months to +25°C in the warmest months, and a minimum temperature ranging from –24°C in the coldest months to +13°C in the warmest months (Figure 3.3).

- In the northern Manitoba region (Thompson and The Pas) the climate is classified as having a total monthly precipitation ranging from +21 mm during the driest months to +90 mm in the wettest months, and a maximum temperature ranging from –20°C in the winter months to +23°C in the summer months, and a minimum temperature ranging from –31°C in the winter months to +12°C in the summer months (Figure 3.4).

In general, the Northwestern Ontario region is the wettest region, the northern Manitoba region is the coldest region, and the southern Manitoba region is the warmest.

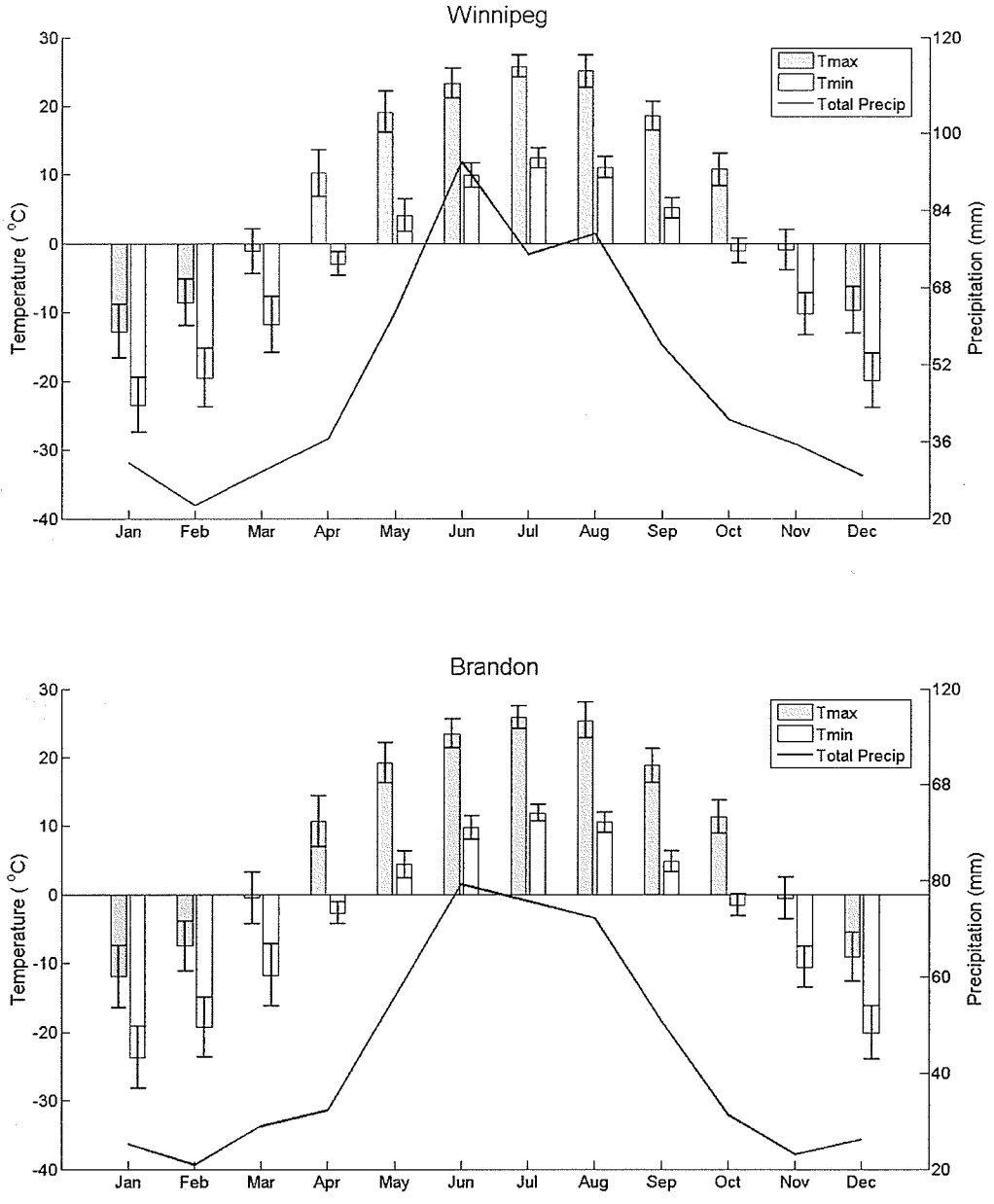

Figure 3.2: Baseline climate (1961-1990) for Winnipeg and Brandon (error bars represent standard deviation)

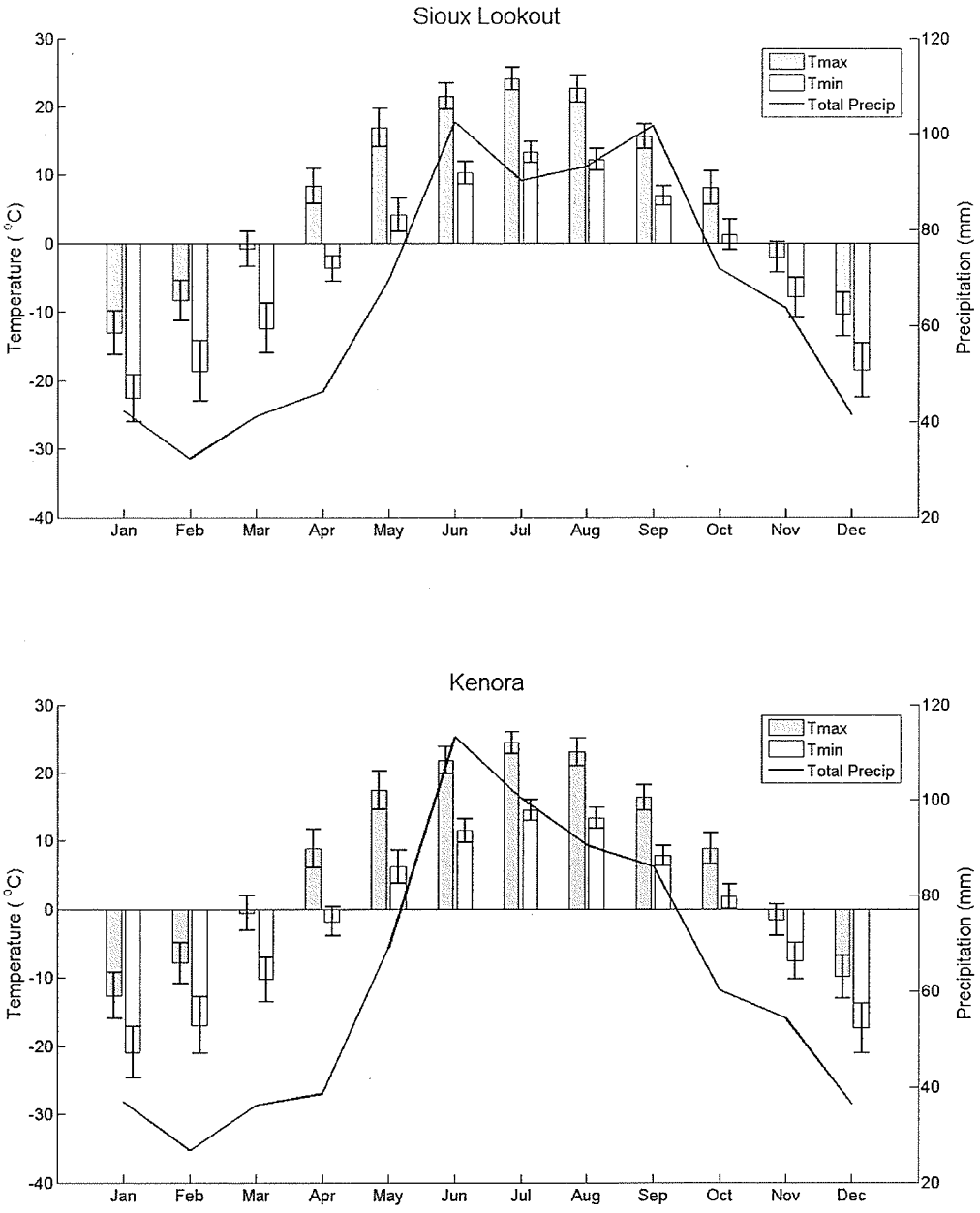

Figure 3.3: Baseline climate (1961-1990) for Sioux Lookout and Kenora Brandon (error bars represent standard deviation)

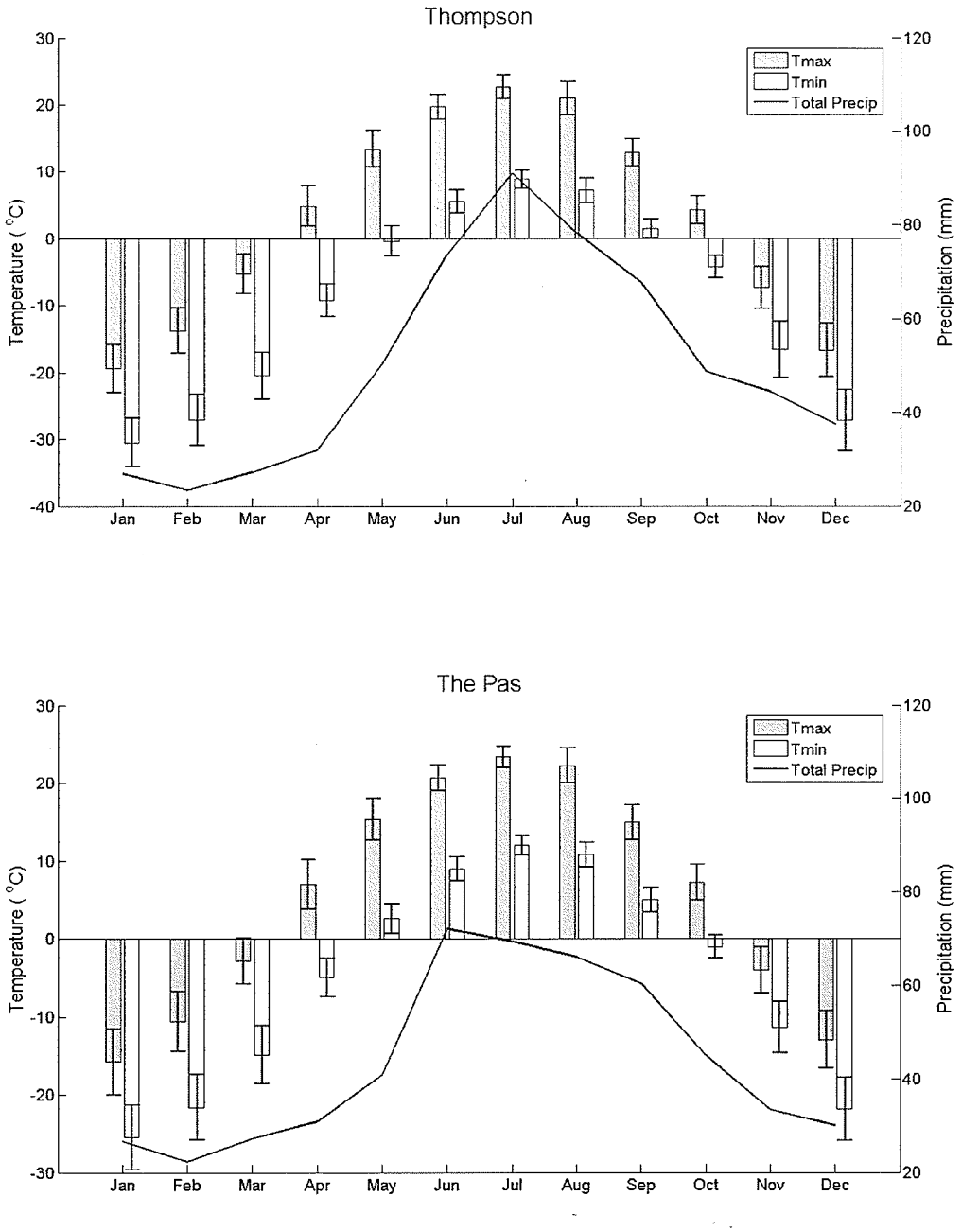

Figure 3.4: Baseline climate (1961-1990) for Thompson and The Pas Brandon (error bars represent standard deviation)

3.2 Data

For the stations selected, three types of daily data were compiled for the purpose of statistical downscaling: (1) observed station data; (2) NCEP reanalysis data; and (3) GCM simulations of current and future climate.

3.2.1 Meteorological Data

The Environment Canada meteorological dataset for daily homogenized maximum and minimum temperature (hereafter called Tmax and Tmin) prepared by Vincent et al. (2002) and the daily adjusted total precipitation dataset prepared by Mekis and Hogg (1999) were used in this study. Due to the different behavior of climate variables, different approaches were applied for homogenization of temperature and precipitation. For temperature, a statistical technique was first applied to identify all of the potential inhomogeneities. The associated cause of each of the inhomogeneities was then identified by retrieving the information through the historical reports. For precipitation, since the Canadian network density of precipitation gauges is so sparse, there is insufficient information to allow widespread use of surrounding station data to identify and adjust inhomogeneities. Therefore, in the case of precipitation the objective was to correct the measurements such as instrument changes, snow density differences, gauge under-catch, and trace measurements for all known inhomogeneities. These data sets were selected in order to minimize the risk of introducing additional uncertainty from the relocation of stations and from changes in climate monitoring practices.

Table 3.2: Predictor variables

No.	*Predictor Name*	*No.*	*Predictor Name*
1	Surface airflow strength	14	850hpa zonal velocity
2	Surface zonal velocity	15	850hpa meridional velocity
3	Surface meridional velocity	16	850hpa vorticity
4	Surface vorticity	17	850hpa wind direction
5	Surface wind direction	18	850hpa divergence
6	Surface divergence	19	Mean sea level pressure
7	500hpa airflow strength	20	500 hpa geopotential height
8	500hpa zonal velocity	21	850hpa geopotential height
9	500hpa meridional velocity	22	Specific humidity at 500hpa
10	500hpa vorticity	23	Specific humidity at 850hpa
11	500hpa wind direction	24	Near surface specific humidity
12	500hpa divergence	25	Mean temperature at 2m
13	850hpa airflow strength		

3.2.2 National Center for Environmental Prediction (NCEP)

Climate predictors were derived from the National Center for Environmental Prediction (NCEP/NCAR) (hereafter called NCEP) reanalysis data set (Kalnay et al. 1996). Twenty five potential downscaling predictor variables were extracted or derived from the daily grid point output of the NCEP reanalysis (Table 3.2).

Mean sea level pressure (mslp), 500 hPa, and 850 hPa geopotential heights (z500 z850), mean daily temperatures 2 m above the land surface (Temp2m), specific humidity at the surface, 500hPa, and 850 hPa (RH, RH500, RH850), were extracted from the daily grid point output of the NCEP reanalysis for the grid point closest to a station.

Six upper-atmosphere variables were derived from z500 and z850: zonal and

meridional velocity components, strength of the resultant flow, vorticity, and divergence. Five surface variables were derived from mslp: zonal and meridional components of airflow velocity, strength of the resultant flow, vorticity, and divergence (Choux 2005; Gachon et al. 2008- see Appendix A).

All variables were re-gridded from the NCEP grid (2.5° latitude by 2.5° longitude) to the CGCM3 T47 grid (approx. 3.75°latitude by 3.75°longitude) (Section 3.2.3) and then standardized. The re-gridding was required since the grid spacing of the NCEP dataset used for the statistical downscaling calibration does not correspond to the grid spacing of the GCM output (Figure 3.1). The standardization which consisted of subtracting the monthly mean and dividing by the monthly standard deviation for a predefined baseline period (1961-1990) was used to reduce biases in the mean and variances of the atmospheric fields relative to observations (Wilby et al. 2004).

3.2.3 Third Generation Canadian Global Climate Model (CGCM3)

The Canadian Center for Climate Modeling and Analysis (CCCma) (http://www.cccma.bc.ec.gc.ca/) provides GCM daily data for a number of surface and atmospheric variables for the CGCM3 T47 version which has a horizontal resolution of roughly 3.75° latitude by 3.75° longitude and a vertical resolution of 31 levels. CGCM3 is the third version of the CCCma Coupled Global Climate Model which makes use of a significantly updated atmospheric component AGCM3 and uses the same ocean component as in CGCM2 (http://www.cccma.ec.gc.ca/models/cgcm3.shtml).

Data was obtained for CGCM3 climate of the 20th Century (20CM3) experiments and the IPCC Special Report on Emission Scenarios (SRES) A1B, A2 and B1 scenarios for two future decadal periods (Figure 5.1). The SRES series are characterized as (IPCC 2000):

- SRESA1B: The A1B scenario (A1B) is a subset of the A1 family in which the technological emphasis is a balance between all energy sources (fossil-fuels and non-fossil energy sources). The A1 family is characterized by rapid economic growth, the quick spread of new and efficient technologies and a global population, which peaks by 2050 and declines after.
- SRESB1: The B1 storyline (B1) and scenario family has the same global population as the A1 storyline which peaks by 2050 and then declines. However, it has a rapid change towards an information and service economy with the introduction of clean and resource-efficient technologies and a reduction in material intensity. There is an emphasis towards global solutions to social, economic, and environmental sustainability.
- SRESA2: The A2 storyline and scenario family (A2) is a more divided world with self-reliant nations and a continuously increasing global population. The economic development is regionally oriented and there are slower, more fragmented technological changes and per capita economic growth.

Tmax, Tmin, and precipitation were extracted from the daily grid point output of

the CGCM3 for the grid point closest to each station. In addition, the same predictor variables as those obtained from NCEP were extracted and derived except in this case no re-gridding of the data was required. CGCM3 predictor variables were standardized with respect to their 1961-1990 monthly mean and monthly standard deviation for both the current and future periods.

Chapter 4

Solar Radiation

4.1 Introduction

Historical meteorological data sets often have missing records. This poses a problem for models that require inputs of missing variables. For example, many sites across central Canada have not recorded solar radiation which is an input for LARS-WG and is often used in hydrologic models. In order to fill the gaps in missing records, certain weather generators have been developed to derive the missing variables based on the ones that are readily available at the sites.

Climatic Data Generator (ClimGen) is a weather generator that is capable of generating solar radiation data, along with many other meteorological variables, based on variables which are already recorded (Tmax, Tmin, and precipitation) (Nelson 2007). This weather generator has been selected to simulate solar radiation at a series of sites in central Canada.

4.2 Climatic Data Generator (ClimGen): Solar Radiation

Solar radiation is estimated from temperature in ClimGen, using the procedure described by Bristow and Campbell (1984) and modified by Donatelli and Campbell (1998). In this procedure, daily solar radiation (S_t) is estimated from the product of extraterrestrial solar

radiation (S_o) and the daily total atmospheric transmittance (T_t):

$$S_t = T_t S_o \qquad \textbf{Eq. 4.1}$$

where S_o is computed using the method described in Allen (1998), and T_t is given as a function of the daily temperature amplitude (ΔT) as:

$$T_t = A\left[1 - e^{-B\,adj_{Tavg} \bullet (\Delta T)^2\, adj_{T\min}}\right] \qquad \textbf{Eq. 4.2}$$

where A represents clear sky transmissivity, B is a fitted-parameter computed using ΔT, and ΔT is the temperature amplitude computed as (Bristow and Campbell 1984):

$$\Delta T = T_{max_i} - \frac{T_{\min_i} + T_{\min_{i+1}}}{2} \qquad \textbf{Eq. 4.3}$$

where the subscript i is a daily index. The terms adj_{Tavg} and adj_{Tmin} are adjustment factors that are functions of daily average and minimum temperatures, respectively. These are given by Donatelli and Campbell (1998):

$$adj_{Tavg} = 0.017e^{(e^{-0.053T_{avg}})} \qquad \textbf{Eq. 4.4}$$

$$adj_{T\min} = e\frac{T_{\min}}{T_{nc}} \qquad \textbf{Eq. 4.5}$$

The values of A, B, and T_{nc} are determined from observed weather data. The clear-sky transmissivity, A, is determined as the average S_t/S_o, ratio for clear days in the database. Once the value of A is determined, the parameters T_{nc} and B are optimized to minimize the error of estimated versus measured S_t values.

4.3 Sites for Evaluation

Three sites were selected to evaluate ClimGen on its ability to generate solar radiation (Table 4.1). These sites have a sufficient amount of solar radiation data recorded to

Table 4.1:Sites for evaluation of ClimGEN

Station Name	*Latitude (°N)*	*Longitude (°W)*	*Elevation (m)*	*Years of Record*
The Pas A	53.97	–101.10	270	49
Thompson A	55.80	–97.87	222	32
Winnipeg A	49.92	–97.23	239	47

compare the observed records with the simulated values.

4.4 Methodology

The following statistical indices were used to evaluate the generated solar radiation data against the observed values at the sites:

The root mean squared error (RMSE) calculated as:

$$RMSE = \sqrt{\frac{\sum_{i=1}^{n}(O_i - E_i)^2}{n}} \qquad \textbf{Eq. 4.6}$$

where n is the number of values, and O_i and E_i are the i^{th} observed and estimated values. The lower limit of RMSE is 0, indicating perfect agreement between the observed values and the generated values.

The relative error (RE):

$$RE = \frac{RMSE}{\overline{O}} \qquad \textbf{Eq. 4.7}$$

where $\overline{O}$ is the mean of the observed data. The lower limit of RE is 0, indicating perfect agreement between generated and observed values.

The Willmott (1982) index of agreement (d):

$$d = 1 - \frac{\sum_{i=1}^{n}(E_i - O_i)^2}{\sum_{i=1}^{n}\left(\left|E_i'\right| + \left|O_i'\right|\right)^2} \qquad \textbf{Eq. 4.8}$$

where $E_i' = E_i - O$ and $O_i' = O_i - O$. The index of agreement d ranges between 0 and 1, where a value of 1 indicates perfect agreement.

The coefficient of determination (R^2) of the regression between observed and estimated values, with $R^2 < 0.85$ considered as poor.

Box plots and bar charts were also developed to visually compare the generated results with the observed data.

4.5 Results and Discussion

The statistics used to evaluate the simulated daily solar radiation with the observed values for the three sites are shown in Table 4.2. Box plots which compare the simulated solar radiation with the observed data on a monthly scale are shown in Figure 4.1. Bar plots of the mean monthly solar radiation at the each site are shown in Figure 4.2 to Figure 4.4.

The values in Table 4.2 show that the observed mean over the 1961-1990 period compares closely with the values generated from ClimGen. The RMSE and RE are close to zero indicating good agreement between the simulated and observed values. Finally, the Willmot index (d) and the R^2 are both close to one, again indicating good model agreement between the simulated and observed values at all three sites.

The box plots and bar plots for Thompson, The Pas, and Winnipeg (Figure 4.2 to

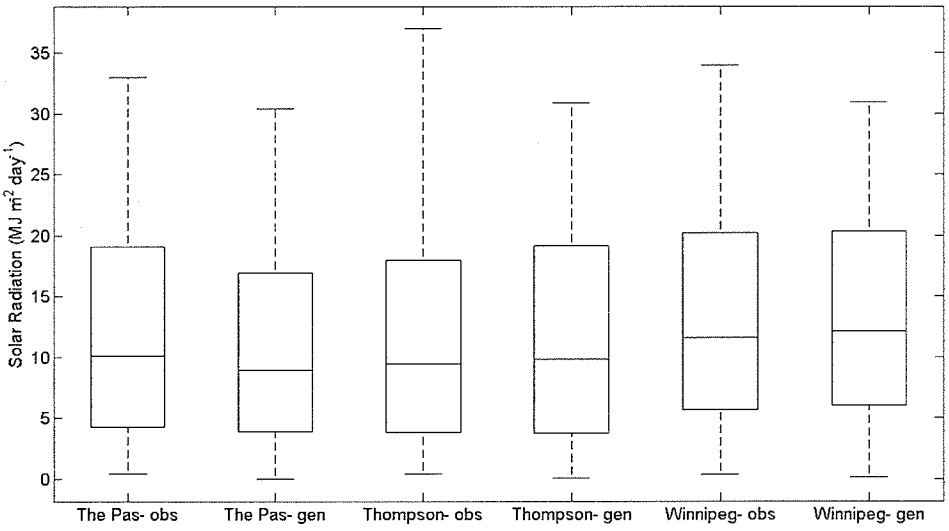

Figure 4.1: ClimGen boxplots

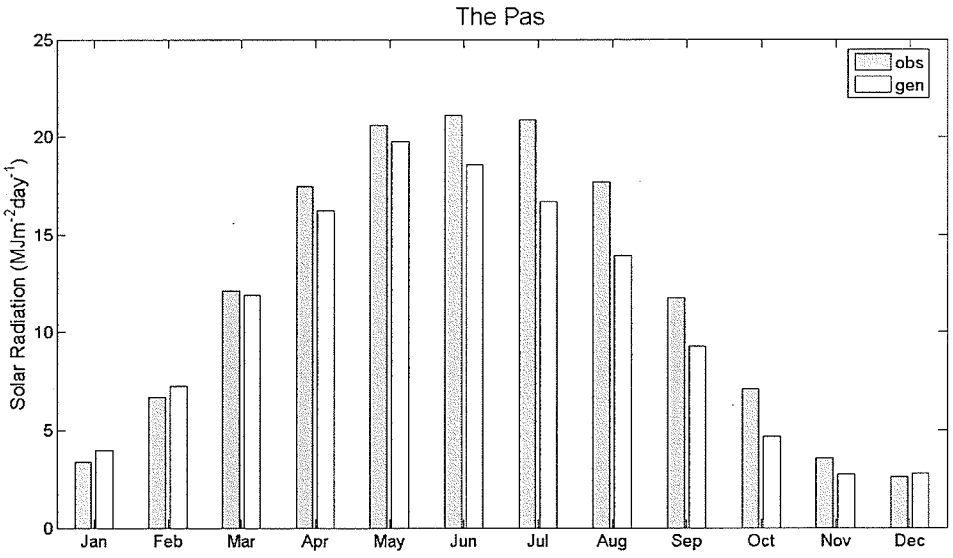

Figure 4.2: ClimGen monthly bar plots at The Pas

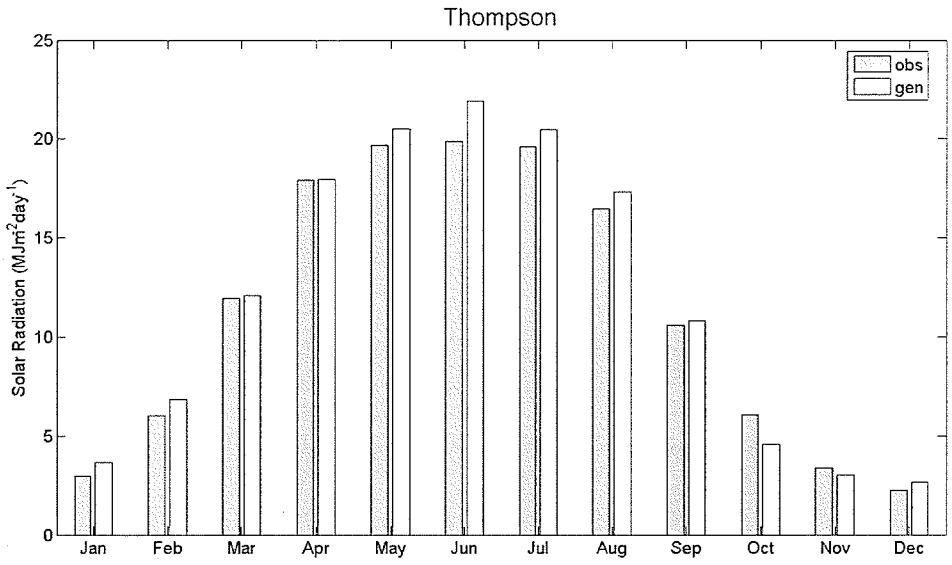

Figure 4.3: ClimGen monthly bar plots at Thompson

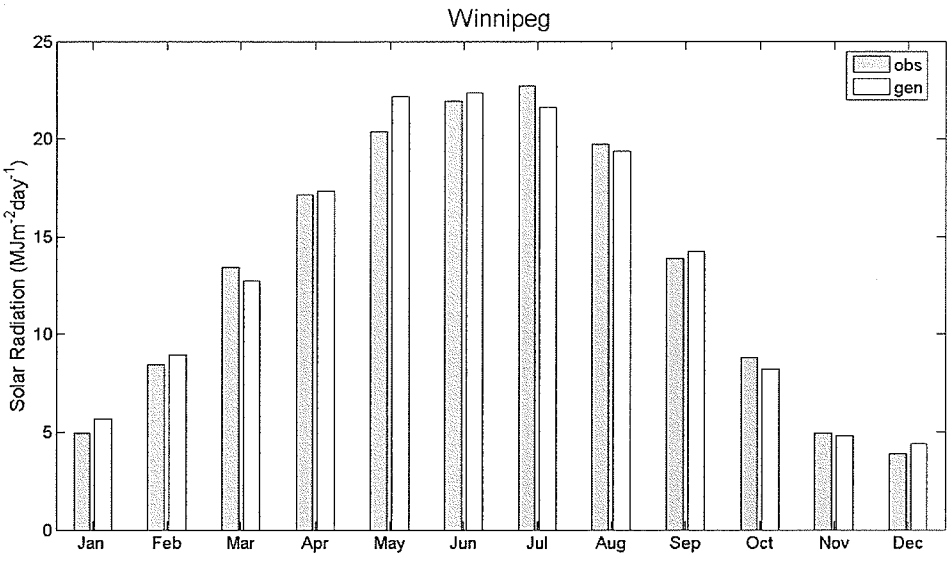

Figure 4.4: ClimGen monthly bar plots at Winnipeg

Table 4.2: Statistics from ClimGEN

Station Name	*Mean (Obs)*	*Mean (Gen)*	*RMSE*	*RE*	*d*	R^2
The Pas A	12.0410	10.7789	0.2351	0.0195	0.9994	0.8781
Thompson A	11.4232	11.8568	0.2707	0.0237	0.9868	0.9079
Winnipeg A	13.2853	13.4432	0.2627	0.0198	0.9536	0.8916

Figure 4.4), all show good agreement between the simulated solar radiation values from ClimGen and the observed data.

4.6 Conclusions

The results show that ClimGen is capable of generating solar radiation data with values similar to the observed records at the Thompson, The Pas, and Winnipeg stations. It can be concluded that ClimGen is suitable to generate missing solar radiation at sites in central Canada where values of Tmax, Tmin, and precipitation are recorded. Based on this analysis, ClimGen is used in this study to generate solar radiation at the Kenora and Sioux Lookout sites where solar radiation data was not recorded.

Chapter 5

Methodology

5.1 Historical Trend Analysis

Recent changes in the mean and variance (climatic trends) of temperature and precipitation can provide useful information for some impact and adaptation studies. Climatic trends may be identified in historical climate records provided that the records cover a long enough period of time (typically more than 100 years). In Canada much of the observational network in the north was not established until the late 1940s and is very sparse. In addition, the observational network has changes in station locations, in instrumentation, and in observing practices that have caused heterogeneities in the climate records. Reliable trend estimates cannot be made before these heterogeneities issues are adequately resolved. A recently created database of temperature (Vincent and Gullet, 1999) and precipitation (Mekis and Hogg, 1999) which attempts to remove these heterogeneities was used in this study for the period of 1941-2000. The relatively short time frame of observations in Canada interferes with the proper identification of statistically significant trends. Nevertheless the data available can be used as a first attempt to examine climatic trends.

First, the Mann-Kendall trend test is applied to determine the direction of any

trend and its significance, and then the Sen Slope Estimator is used to assess the magnitude of the observed rates. Details of these two methods are as follows:

- The non-parametric Mann-Kendall test for trend has a null hypothesis that there is no temporal trend in the data values (H_o: no trend). It is based on the statistic S which is the difference between the numbers of pairwise slopes that are positive minus the number that are negative. Each pair of observed values (y_i, y_j), $i > j$ of the random variables is inspected to determine the number P of cases where $y_i > y_j$ and the number M of cases where $y_i < y_j$. Let S be defined as $S = P - M$, and the test statistics Z as:

$$Z = \begin{cases} (S-1)/\sigma_s & \text{if } S > 0 \\ 0 & \text{if } S = 0 \\ (S+1)/\sigma_s & \text{if } S < 0 \end{cases} \qquad \textbf{Eq. 5.1}$$

where σ_s:

$$\sigma_s = \sqrt{\frac{n(n-1)(2n+5)}{18}} \quad \text{(no ties)} \qquad \textbf{Eq. 5.2}$$

$$\sigma_s = \sqrt{\frac{1}{18}[n(n-1)(2n+5) - \sum_{p=1}^{g} w_p(w_p-1)(2w_p+5)]} \quad \text{(ties occur)} \qquad \textbf{Eq. 5.3}$$

where: g represents the number of tied groups, w_p represents the number of data points in the p^{th} group, and n represents the sample size.

When the sample size (n) is greater than 10, the test statistics (Z) approximately follows the standard normal distribution. The hypothesis H_o (no trend) is rejected at a 5% significance level against the alternatives:

- Ho: no trend
- H_1: trend (with no sign) - reject H_o if $|Z| > z_{0.975}$
- H_2: (an upward trend) - reject H_o if $Z > z_{0.95}$
- H_3: (a downward trend) - reject H_0 if $Z < z_{0.05}$

- The non-parametric Sen Slope Estimator which is insensitive to outliers is computed to quantify the magnitude of trend. The slope b_{ij} is first computed between each possible pair of data points (x_i, y_i) and (x_j, y_j).

$$b_{ij} = \frac{y_i - y_j}{x_i - x_j} \qquad \textbf{Eq. 5.4}$$

The trend estimate is the median of all the pairwise slopes. If there is no underlying trend, the median would be near zero indicating approximately the same number of negative and positive slopes (USEPA 2006).

5.2 Statistical Downscaling

GCMs have uncertainties related to parameterization schemes and model structures as described in Section 2.3.2. As a result of these uncertainties, GCMs vary in their accuracy in reproducing observed atmospheric and surface variables across space and time (Gachon et al. 2005). In a comprehensive climate impact study, the skill of any downscaling model must be tested using a variety of climatic conditions as well as a

range of GCMs. Three climatic regions in central Canada were selected for this study and are described in Section 3.2.3. Due to limited GCM data availability, only one climate model experiment CGCM3 was selected for evaluation.

A GCMs ability to simulate near surface variables (predictands) should be performed at the start of climate impact studies to identify the potential value gained from downscaling. Therefore, after a set of downscaling results have been developed, the value added from downscaling relative to the raw GCM output should be evaluated.

Verification of the GCMs ability to simulate upper atmospheric variables (predictors) is required prior to any downscaling using SDSM. The verification should identify predictors that have a large bias when compared to NCEP and which should be removed prior to downscaling. The choice of predictor variables is one of the most significant steps in the development of the SDSM. In this study, the predictors were selected as follows:

1) The explained variances of all predictors were derived in groups of approximately six to eight at a time. In each group typically one to three predictors had the highest explained variance and were set aside.

2) All the predictors set aside were then assessed to see how correlated they were with each other. This was done since there were instances when predictors had a high explained variance but were also highly correlated with other predictors. A specific predictor will not necessarily add information if it is highly correlated

with other predictors.

3) Scatterplots were developed between the predictors and predictands. This was a visual inspection to indicate the nature of the relationship (i.e. linear) and whether or not any transformations were required.

4) Typically no more than six predictors were selected since any additional ones over this do not add to the model processes in a significant way.

5) The final selected predictors were a combination of moisture variables, circulation variables, and surface temperatures as described in Section 2.5.

Prior to constructing climate change scenarios with SDSM and LARS-WG, the models were evaluated by their ability to simulate mean observed climatic conditions as well as extremes of both temperature and precipitation. According to Wilby et al. (2004), statistical downscaling methods are often calibrated in ways that are not particularly designed to handle extreme events which are critical in some impact studies. Fourteen indices were selected to evaluate SDSM and LARS-WG based on their ability to simulate mean observed climate conditions and extreme events (Table 5.1). These were based on indices used by the Expert Team on Climate Change Detection Monitoring and Indices (http://cccma.seos.uvic.ca/ETCCDMI/software.shtml) (RClimdex), in the European Statistical and Regional Dynamical Downscaling of Extremes for European Regions (http://www.cru.uea.ac.uk/projects/stardex/) (STARDEX), and in various other studies (Gachon et al. 2005; Mekis and Vincent 2005).

Table 5.1: Evaluation indices

	Precipitation Basic Variables	
Mean	Precip. (mean)	Mean precipitation (mm/day)
Standard Deviation	Precip.(std)	Standard deviation of precipitation (mm/day)
	Precipitation Extreme Indices	
Extremes	Rx5	Greatest 5 days total rainfall
	CDD	Consecutive dry days
	R95pTOT	95th percentile of rainday amounts
	Temperature Basic Variables	
Mean	Tmin (mean)	Mean minimum temperature
	Tmax (mean)	Mean maximum temperature
Standard Deviation	Tmin (std)	Standard deviation of minimum temperature
	Tmax (std)	Standard deviation of maximum temperature
	Temperature Extreme Indices	
Daily variability	DTR	Average diurnal temperature range
Cold extremes	Tmin10pb	10th percentile of daily min temperature
	Tmax10pb	10th percentile of daily max temperature
Warm extremes	Tmin90pb	90th percentile of daily min temperature
	Tmax90pb	90th percentile of daily max temperature

For LARS-WG, data from 1961-1990 was used for the calibration of the model and to establish the parameter file. One hundred series of synthetic values were then generated for verification to compare with observed climate data indices (Table 5.1).

For the calibration of SDSM, predictors from NCEP (1961-1990), interpolated onto the CGCM3 grid, were used. After the model was calibrated, predictors from the calibration period were used to generate 100 ensembles of synthetic daily values for verification purposes and these simulations were compared with observed climate using the indices described in Table 5.1. To ensure consistency with LARS-WG, 100 series of synthetic ensembles was generated by SDSM and the ensemble with the highest

correlation to the overall ensemble median was selected. Once SDSM was calibrated using NCEP predictors, similar ensembles of synthetic variables using predictors from CGCM3 were generated.

After the calibration and evaluation of SDSM and LARS-WG over the 1961-1990 period both models were validated on an independent time period from 1991-2000. For SDSM, a set of predictor variables over the 1991-2000 period were inputted into the model and the predictands were generated. For LARS-WG, the observed station data over the 1991-2000 time period was used to develop a parameter file to capture any climatic characteristics unique to the 1991-2000 period. The difference between this parameter file and the parameter file over the baseline period (1961-1990) was then used to develop a 1991-2000 scenario file which was used to generate climate data.

5.2.1 Criteria to Evaluate Statistical Downscaling

The predictands (Tmax, Tmin, and precipitation) were analyzed by comparing the simulations from SDSM and LARS-WG with observed station data, focusing on simulated monthly/seasonal means and selected extreme indices (Table 5.1).

The bias is computed by comparing the observed and simulated values as follows:

$$B = \overline{O} - \overline{S} \qquad \textbf{Eq. 5.5}$$

where: B is the bias, $\overline{O}$ is the monthly or seasonal mean of the observed variable, and $\overline{O}$ is the monthly or seasonal mean of the simulated variable.

Graphical techniques (Q-Q plot, probability density function plots, and box plots) were also used to evaluate the downscaling results:

- Probability density function plots (PDFs) were used to determine the overall fit of SDSM-NCEP, SDSM-CGCM3, LARS-WG and the raw CGCM3 data compared to the observed data.
- Quantile-quantile (Q-Q) plots were used to compare the modeled distribution with the distribution of observed data. Q-Q plots were developed for Tmax, Tmin, and precipitation at all the stations in order to analyze the fit of the modeled distributions from SDSM-NCEP, SDSM-CGCM3, and LARS-WG. In addition, raw CGCM3 outputs were plotted to demonstrate the GCM's skill at simulating current climate and the added value from downscaling. When constructing a Q-Q plot, the quantiles of one dataset are plotted against the quantiles of another data set. A 45 degree reference line is plotted along with the quantiles. In theory, if the data sets come from the same distributions, points should fall approximately along this reference line.
- Box plots were used to assess the agreement of distributions modeled by SDSM-NCEP, SDSM-CGCM3, and LARS-WG with the observed distribution of Tmax, Tmin, and precipitation as well as all the extreme indices. In addition, box plots with raw CGCM3 outputs for Tmax, Tmin, and precipitation were plotted to evaluate the GCM's skill and the value gained from downscaling. A box plot illustrates the spread of a data around

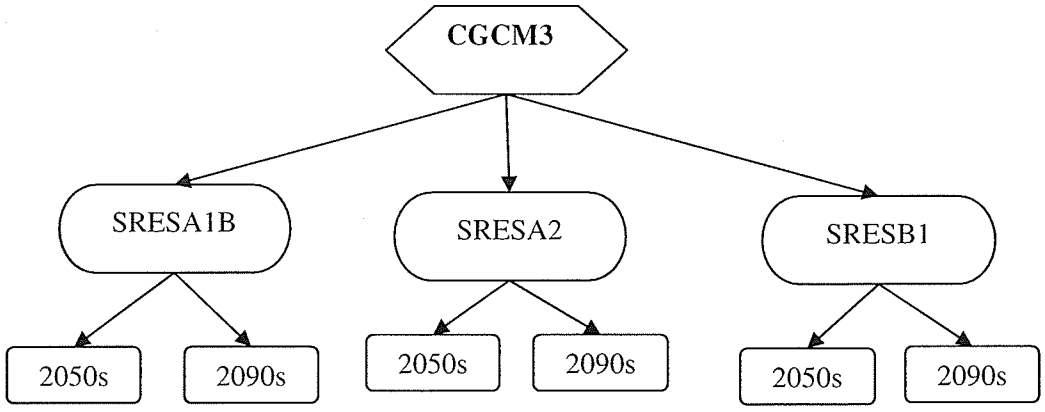

Figure 5.1: CGCM3 emission scenarios and time periods

the median value. If simulated box plot range values fall outside the range of the box plot constructed for the observed values, it indicates that the model is underestimating or overestimating the true values.

5.3 Climate Change Scenarios

Once it has been confirmed that SDSM and LARS-WG were capable of simulating current climate with some degree of skill, they could be used to construct climate change scenarios. Using the data available from CGCM3, three future emissions scenarios (SRESA1B, SRESA1, SRESB1) at each of the sites in the study area are applied for two future time periods (2050s and 2090s) to construct climate change scenarios (Figure 5.1). This allows for an ensemble of climate change scenarios at each site for use in an impact model.

In order to construct climate change scenarios with LARS-WG, the parameter file

established for current climate must be perturbed according to the specific SRES and time period. The methodology to perturb this file can be found in Section 2.7. The model is then able to simulate future climate change scenarios at the site. Constructing climate change scenarios using SDSM involves applying GCM predictors from one of the SRES/time periods to the calibrated SDSM.

Chapter 6

Results and Discussion

6.1 Historical Trend Analysis

6.1.1 Temperature

The seasonal mean temperature trend analysis over 1941-2000 concluded that trends vary for different regions and for different seasons. The number of stations with statistically significant trends in Tmax, Tmin, and Tmean are presented in Table 6.1. Strong warming is the main characteristic of the mean seasonal Tmax, Tmin, and Tmean as there were no negative trends found. Among the four seasons, spring showed the greatest warming in the south for Tmax, Tmin, and Tmean (approximately +1.97°C for Tmean). While in the north the winter season showed the greatest warming for Tmax, Tmin, and Tmean (approximately +2.04°C for Tmean). In all regions no significant trends were found for the autumn season. For the standard deviations in each region, no general conclusions can be drawn regarding trends. These results are consistent with those found by Zhang et al. (2000) who studied trends across Canada. They found that spring showed the greatest warming, with winter also showing a warming.

6.1.2 Precipitation

Statistically significant trends of mean precipitation and standard deviation are shown in

Table 6.1: Number of sites and direction of statistically significant temperature trends (+ is a positive trend – is a negative trend). SE: Southeast region- Kenora and Sioux Lookout, SW: Southwest region- Winnipeg and Brandon, NE: Northeast region- Thompson and The Pas.

	Winter			*Spring*			*Summer*			*Autumn*		
	SE	**SW**	**NE**	**SE**	**SW**	**NE**	**SE**	**SW**	**NE**	**SE**	**SW**	**NE**
Tmax	0	0	+2	+2	+2	+1	0	0	+1	0	0	0
Tmean	+1	0	+1	+2	+2	+1	+2	+1	0	0	0	0
Tmin	+2	0	+2	+2	+2	0	+2	+1	0	0	0	0
Tmax (STD)	0	0	−1	0	0	0	0	0	0	0	0	0
Tmean (STD)	0	0	0	0	0	0	0	+2	0	+1	0	0
Tmin (STD)	0	0	0	0	−1	0	+2	+1	0	+1	0	0

Table 6.2: Number of sites and direction of statistically significant precipitation trends (+ is a positive trend – is a negative trend). SE: Southeast region- Kenora and Sioux Lookout, SW: Southwest region- Winnipeg and Brandon, NE: Northeast region- Thompson and The Pas.

	Winter			*Spring*			*Summer*			*Autumn*		
	SE	**SW**	**NE**	**SE**	**SW**	**NE**	**SE**	**SW**	**NE**	**SE**	**SW**	**NE**
Precip.	−1	0	−1	0	0	0	0	0	0	0	0	0
Precip. (STD)	0	0	+1	0	0	0	0	0	+1	+1	0	+1

Table 6.2. With the exception of two stations which had statistically significant downward trends in precipitation (one in the southeast and one in the northeast) no other sites showed statistically significant trends.

6.2 Third Generation Canadian Global Climate Model Analysis

6.2.1 Predictand Analysis

CGCM3s ability to simulate current climate was evaluated at all six stations by

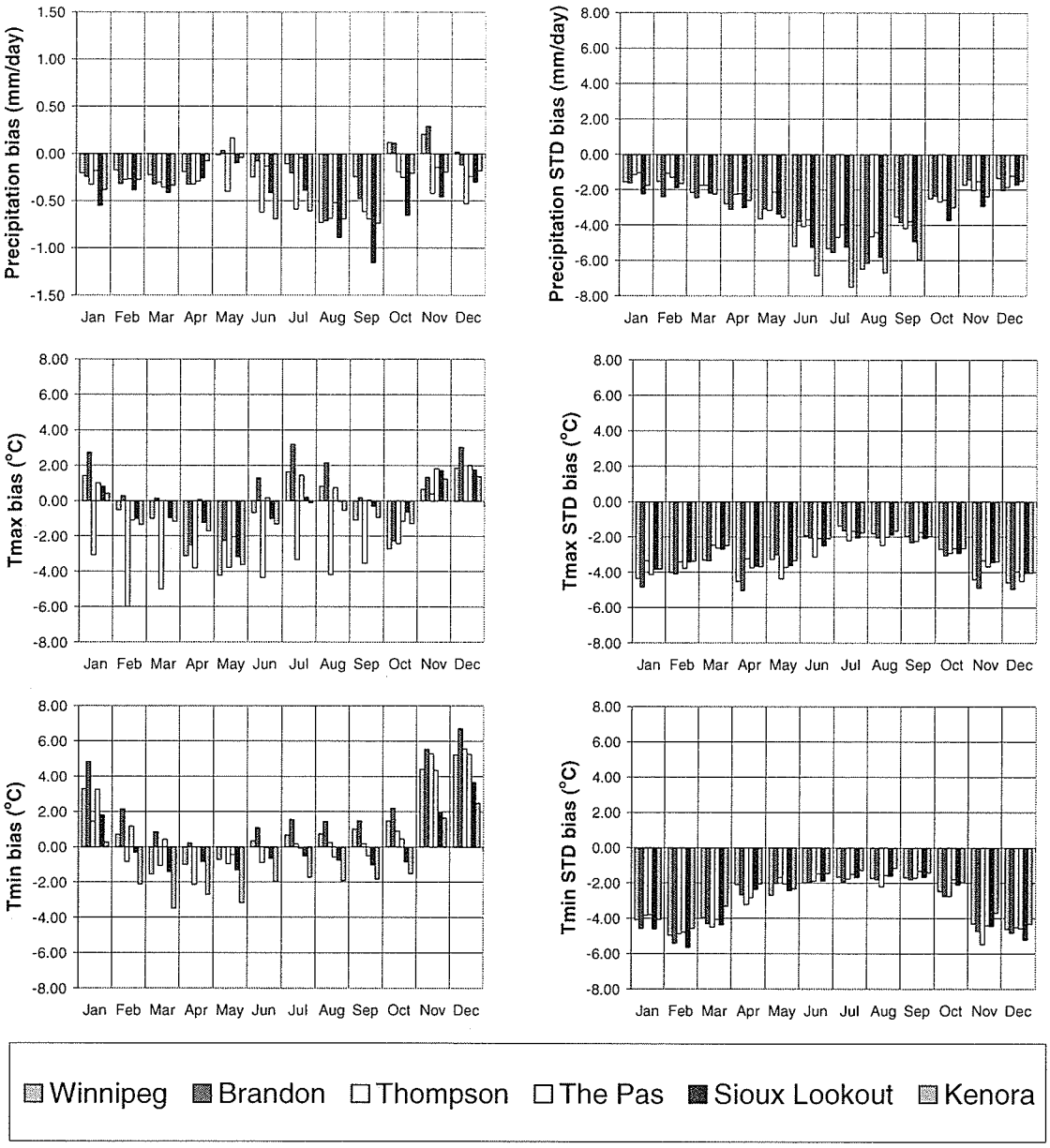

Figure 6.1: CGCM3 simulation monthly bias over the 1961-1990 period

comparison with historical station data over the 1961-1990 time period. The precipitation, Tmax, and Tmin monthly mean and standard deviation bias of CGCM3 is shown in Figure 6.1. With a few exceptions CGCM3 underestimates the monthly mean

precipitation at all stations. On an annual basis, the mean precipitation bias was underestimated by −17% (ranging from −7% at Winnipeg to −28% at Thompson). On a monthly basis the average bias was −0.32 mm/day (−0.15 mm/day to −0.50 mm/day) with August and September having the largest monthly mean bias of −0.68 mm/day. The standard deviation of precipitation was consistently underestimated with an average bias of −3.15 mm/day. June, July, August, and September reported the highest underestimations of the standard deviation bias with an average of −5.06 mm/day. These months are primarily comprised of convective thunderstorms which may not be captured in the GCM simulation due to its coarse spatial scale.

On average the monthly mean of the Tmin and Tmax are over- and under-estimated by approximately +0.66°C (Tmin) and −0.68°C (Tmax). For Tmin, the most significant bias occurs in January, November, and December with an average bias of +3.72°C, and April and May with an average bias of −2.61°C. The standard deviation for Tmin and Tmax is underestimated by an average bias of −2.86°C (Tmin) and −2.99°C (Tmax) with the winter months having the largest bias of −4.59°C for Tmin and for Tmax −3.98°C.

CGCM3 clearly produces poor simulations of the surface variables Tmax, Tmin, and precipitation at all the stations in the study area. The bias is most prominent when examining the monthly standard deviations at each station. This indicates that CGCM3 has too little variability. CGCM3 has poor skill at simulating climate at the individual stations because its grid values represent averages over a large area (approximately

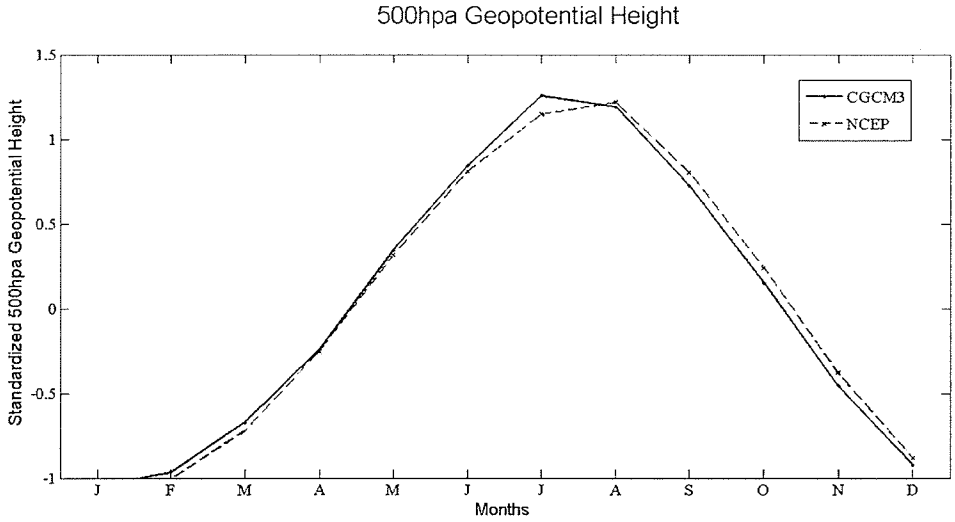

Figure 6.2: 850hpa zonal velocity predictor

300km by 300km) and therefore can not capture much of the variability of the individual stations.

6.2.2 Predictors Analysis for SDSM

As suggested by Wilby et al. (2004), predictors have to be selected based both on their relevance to the downscaled predictands and their ability to be accurately represented by the GCMs. The most favorable predictors must be strongly correlated with the predictand, be physically sensible, and have the ability to capture the climate change signal.

The monthly averages of the standardized CGCM3 and NCEP 500hpa geopotential height predictor are shown in Figure 6.2. Despite the standardization of the GCM predictors, anomalies continue to be exhibited when compared to the corresponding NCEP predictors.

Table 6.2: Selected predictors and R^2 values

Station	*Tmax Predictors*	R^2	*Tmin Predictors*	R^2	*Precipitation Predictors*	R^2
Winnipeg	20, 23, 24, 25	0.78	20, 23	0.69	12, 19, 20, 22, 23	0.20
Brandon	3, 20, 19, 23, 25	0.78	9, 20, 19, 22, 24, 25	0.78	12, 19, 20, 22, 23	0.11
Thompson	20, 22, 23, 24, 25	0.77	20, 22, 23, 24	0.71	2, 9, 18, 22	0.14
The Pas	2, 20, 23, 24	0.76	20, 19, 22, 24	0.71	10, 22, 24	0.11
Kenora	20, 21, 24, 25	0.77	20, 23, 24, 25	0.83	4, 12, 19, 20, 22, 23	0.22
Sioux Lookout	20, 23	0.66	20, 22	0.62	4, 12, 19, 22, 23	0.24

Table 3.2 outlines the list of all candidate predictor variables. The selected predictors for each predictand along with the explained variance are shown in Table 6.2. The explained variance ranges between 0.62 and 0.83 for Tmax and Tmin and between 0.11 and 0.24 for precipitation for all stations. The relatively low explained variance for precipitation underlines the more stochastic nature of precipitation occurrence and magnitude, and the difficulty in capturing the characteristics of the variability of precipitation in the downscaling processes (compared to temperature), as suggested by other studies (Dibike et al. 2007; Gachon et al. 2005).

The predictors chosen for this study were based on a combination of moisture variables, circulation variables, and surface temperatures. This combination was selected to ensure that projected future temperature and precipitation scenarios are realistic by taking into account the processes which may dominate in the future (Section 2.5). This is in agreement with other studies such as Gachon et al. (2005) and Huth (2004), which have shown that the use of categories of predictors is superior to that of predictors from

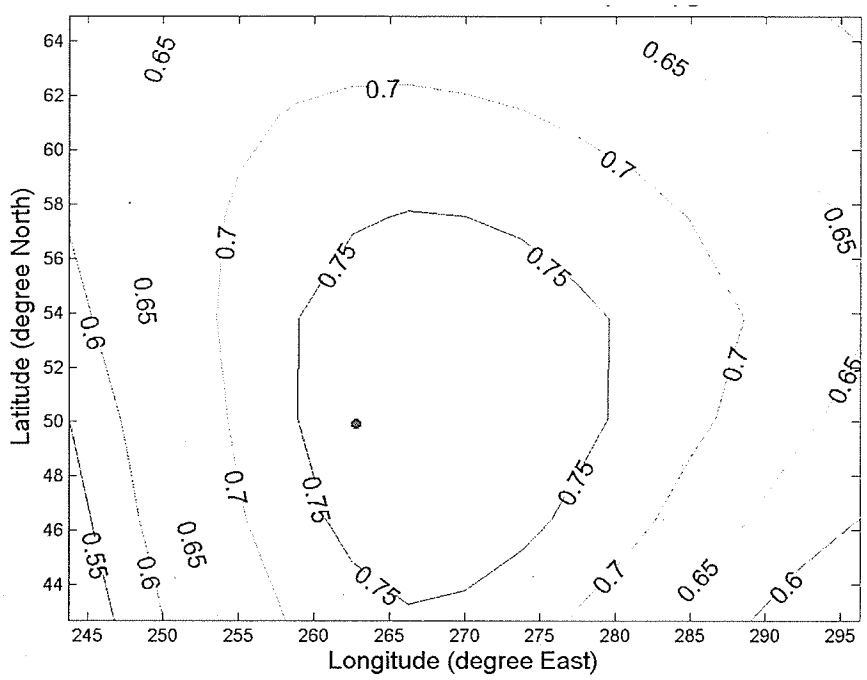

Figure 6.3: Correlation map (Tmin & 500hpa) at Winnipeg

a single category for downscaling temperature and precipitation.

Correlation maps were constructed to determine the optimum location for selection of predictors (Gachon 2007). Figure 6.3 illustrates the predictor variable "500hpa geopotential height" and its correlation with Tmin at the Winnipeg station. This correlation map indicates that the maximum correlation between the predictor and predictand was the grid cell closest to the predictand. Some stations indicate a maximum correlation a few grid points away from the predictands. The difference between the correlation value at this grid point and the one closer to the predictand was too small to produce a significant difference in the performance of the downscaling model. Since the

majority of the maximum correlated grid points were closest to the station of interest, the predictors closest to the grid point of the stations were used for downscaling.

6.3 Downscaling Results

SDSM and LARS-WG were used to generate climate data for six stations described in Section 3.1 (Winnipeg, Brandon, Sioux Lookout, Kenora, Thompson and The Pas). The model outputs (SDSM-CGCM3, SDSM-NCEP, and LARS-WG) were compared with the statistics of observed data of Tmax, Tmin, and precipitation for the calibration period (1961-1990) and the validation period (1991-2000). Evaluation statistics are the means, standard deviations, the selected percentiles (the 95^{th} percentile of rain day amounts, the 10^{th} and 90^{th} percentile of Tmax and Tmin), the maximum number of consecutive dry days, the greatest five day total rainfall, and the average diurnal temperature. In the model evaluation both SDSM-NCEP and SDSM-CGCM3 were tested. Although SDSM-NCEP can not be used for climate change simulations, it is useful to understand how well SDSM performs when provided with NCEP input as opposed to GCM input. This would demonstrate if the simulations degraded when predictors are taken from the GCM rather than NCEP and would highlight potential deficiencies in the GCM predictors which are propagating to SDSM. All the stations in the study area exhibited similar evaluation results and therefore The Pas was used as a representative station. Only evaluation statistics that are significantly different are noted.

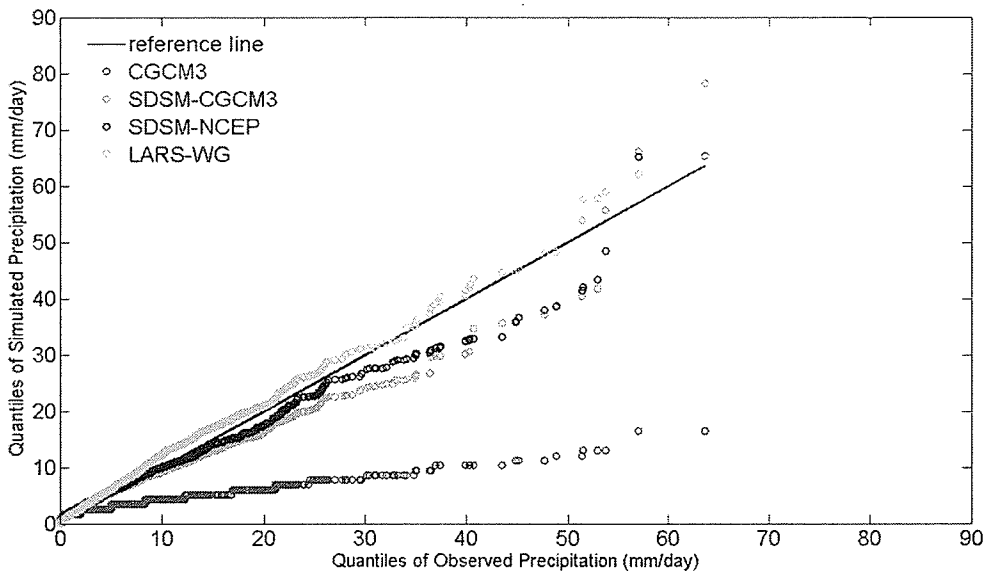

Figure 6.4: Quantile–quantile plots for precipitation (in mm/day) at The Pas (1961-1990)

6.3.1 Calibration Period (1961-1990)

6.3.1.1 Precipitation

A quantile–quantile (Q-Q) plot for observed daily precipitation and raw CGCM3, SDSM-NCEP, SDSM-CGCM3 and LARS-WG output at The Pas is shown in Figure 6.4. The downscaled models (SDSM and LARS-WG) have vastly improved the frequency distribution over the raw CGCM3 model by reducing the underestimation of all percentiles and especially the upper quantiles of daily precipitation. SDSM using CGCM3 predictors generally underestimated the precipitation more than SDSM using NCEP predictors or LARS-WG. Results were similar for the remaining five climate stations (not shown).

Probability density functions (PDFs) are used to compare CGCM3 and the

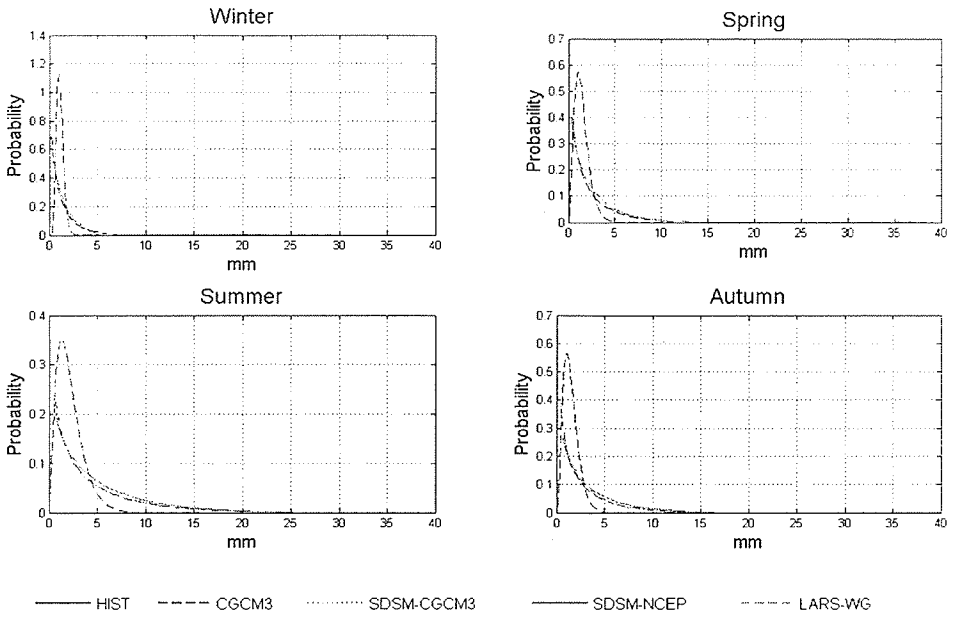

Figure 6.5: Precipitation probability density functions (Gamma Fit) at The Pas (1961-1990)

downscaled precipitation with the observed statistical distribution at The Pas. The PDFs in Figure 6.5 represent the gamma fit distribution to the observed as well as raw CGCM3, SDSM-NCEP, SDSM-CGCM3 and LARS-WG precipitation. The plots show that the downscaled model results all are closer to the observed data than raw CGCM3.

Seasonal daily box plots of precipitation for the calibration and validation periods at Winnipeg, Brandon, Kenora, Sioux Lookout, Thompson, and The Pas were constructed to compare the seasonal mean simulated values with the observed mean. The Pas is presented as a representative station in Figure 6.6. In general, the downscaling results for daily precipitation at each of the six stations reproduce the observed values well. The plots show that LARS-WG, SDSM-NCEP and SDSM-CGCM3 were generally in better agreement with the observed values both for the median, the inter-quartile-range (IQR)

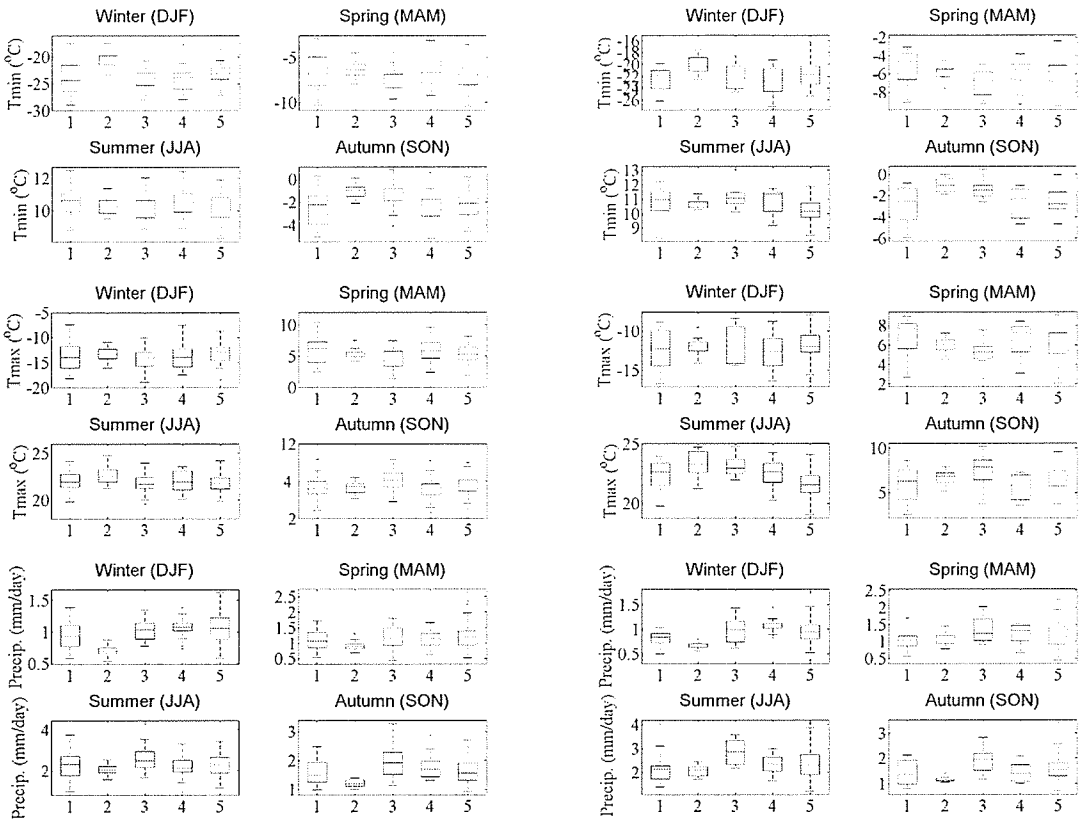

Figure 6.6: Calibration 1961-1990 (left), validation 1991-2000 (right) for Tmin, Tmax and precipitation at The Pas- 1: Historical 2: raw CGCM3 3: SDSM-CGCM3 4: SDSM-NCEP 5: LARS-WG

values and number of outliers than CGCM3. The downscaled information appears to be an improvement over CGCM3 in all seasons and for all stations. The underestimation of the IQR range and extremes from CGCM3 was significantly reduced by downscaling. The IQR and extremes were generally better reproduced on average by LARS-WG, followed by SDSM-NCEP and then SDSM-CGCM3 with no obvious advantage in either of the latter two downscaling techniques. Similar results were obtained on a monthly scale (not shown).

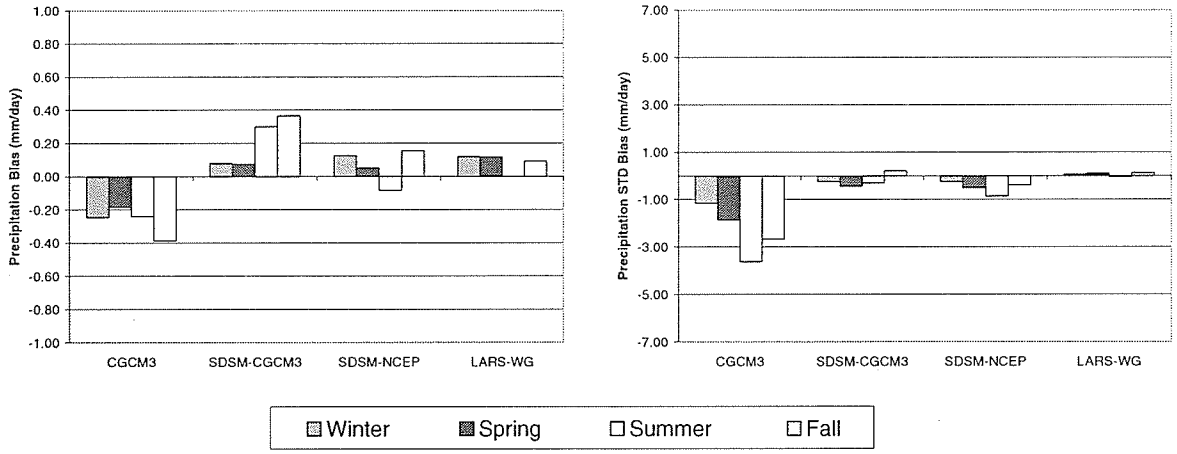

Figure 6.7: Bar plots of bias for seasonal means and standard deviations of precipitation (in mm/day) at The Pas.

The seasonal bar charts of the mean and standard deviation of precipitation at The Pas are presented as a representative sample in Figure 6.7. This figure shows that the precipitation simulated by CGCM3 has a strong bias in most seasons, as CGCM3 underestimates the precipitation for most of the year. Both downscaling models (LARS-WG and SDSM-NCEP) are much closer to the observed values with smaller, generally positive, biases. SDSM with CGCM3 predictors exhibits a larger bias in the summer and autumn. SDSM-NCEP and SDSM-CGCM3 generally underestimate the standard deviation for precipitation. Generally LARS-WG results are closer to the observed values for the standard deviation than SDSM using CGCM3 or NCEP predictors. The results in Figure 6.7 also demonstrate that the statistical downscaling has improved the overall results from CGCM3 by reducing the biases observed in the seasonal mean and standard deviations. Based on the means, there are no significant differences

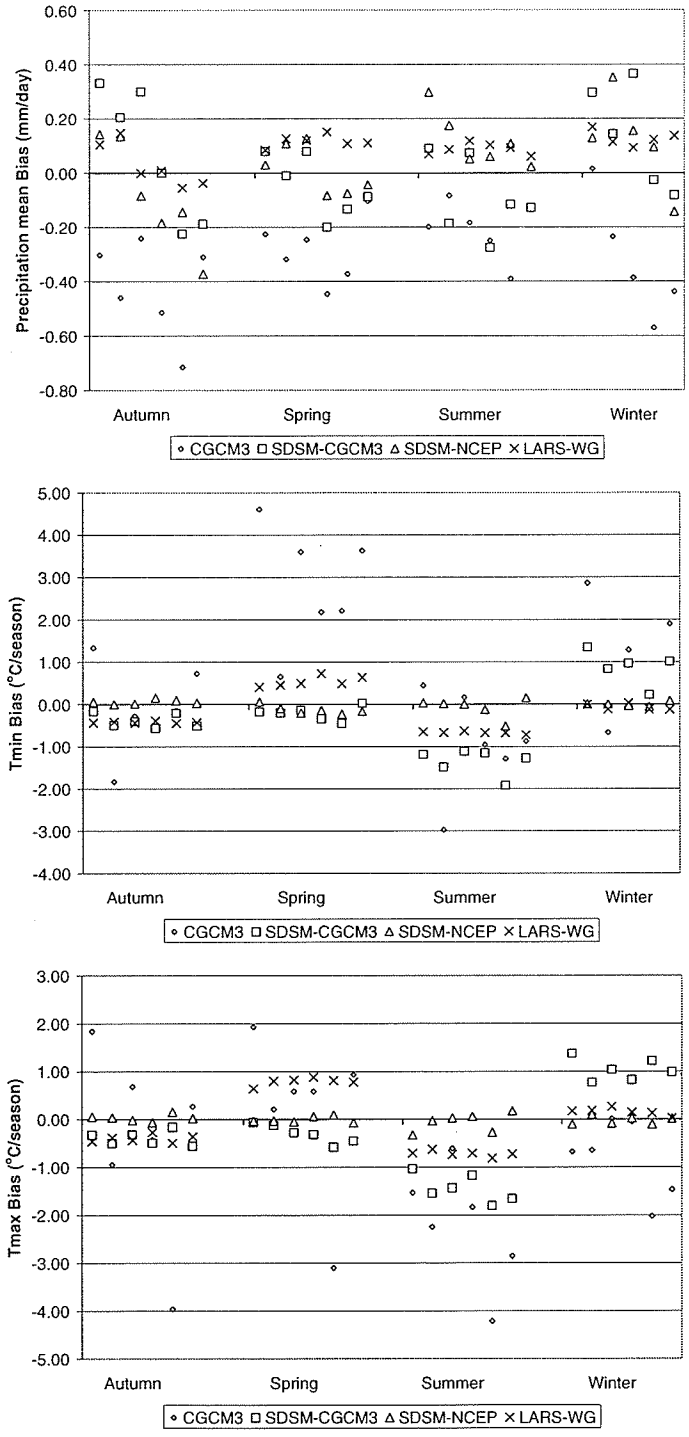

Figure 6.8: Seasonal biases of Tmax, Tmin, and precipitation at each of the six stations (1961–1990). Winnipeg, Brandon, Kenora, Sioux Lookout, The Pas and Thompson correspond to each symbol from left to right for each season.

between the SDSM-NCEP and LARS-WG precipitation results. Similar results were observed on a monthly basis (not shown).

The statistical downscaling performances for precipitation at the six stations in this study are summarized in Figure 6.8. This figure illustrates the relative biases for precipitation, on a seasonal basis, for each station. The results demonstrate that the downscaled data from LARS-WG and SDSM-NCEP give the best performance. Results from SDSM-CGCM3 also have smaller biases than CGCM3 in most of the cases, although there are occasional overestimation of precipitation in autumn and winter and underestimation in the summer. The precipitation from CGCM3 shows significant biases for most of the stations and for most seasons except spring and winter. The results show that SDSM-NCEP and LARS-WG biases are relatively small, while SDSM-CGCM3 biases are usually larger. Generally, there does not appear to be any major difference in the precipitation downscaling performances between stations or seasons or any systemic bias between seasons or models.

Seasonal bar plots are used to compare the raw CGCM3 and downscaled precipitation indices for the 95th percentile, five day total rainfall, and consecutive dry days (CDD) with the observed statistical distribution (Figure 6.9):

- For the 95^{th} percentile indices, CGCM3 generally shows a negative bias while the two downscaled models both show a general moderate positive bias for this index, with the exception of the spring and summer season for SDSM-NCEP. The other five stations reported similar seasonal results for the 95^{th} percentile with

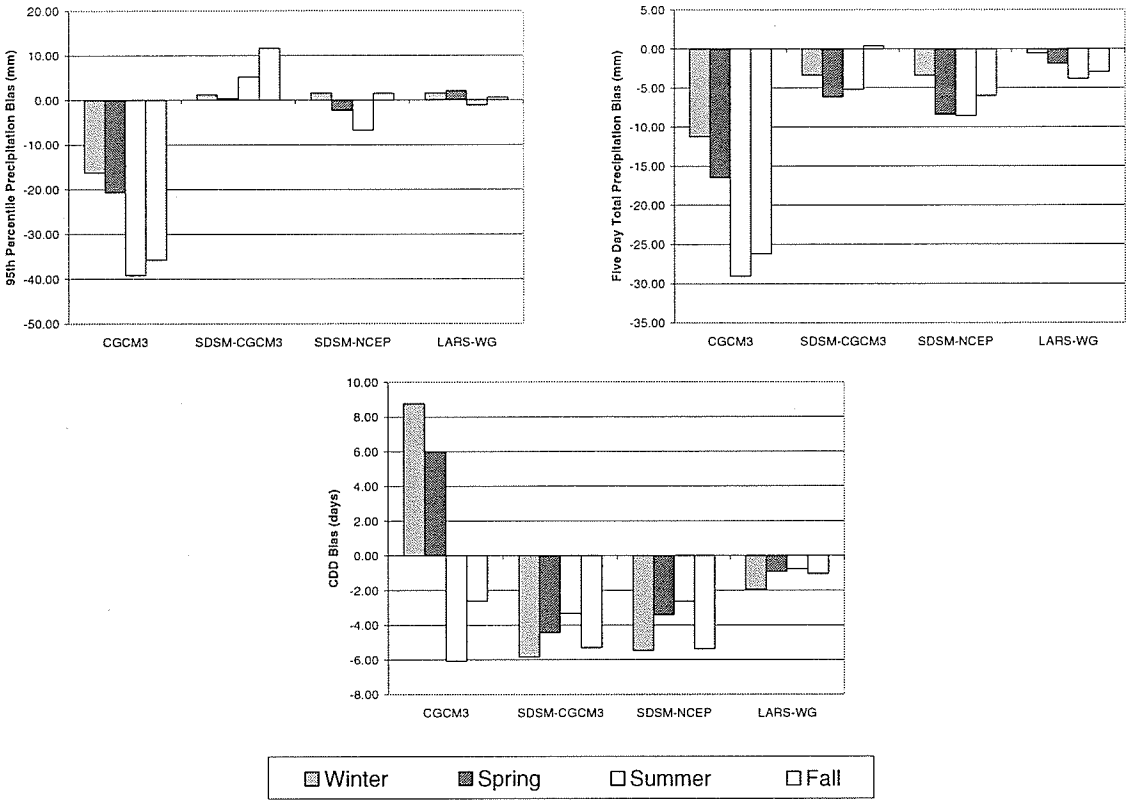

Figure 6.9: Seasonal biases of precipitation indices (5 day total rainfall, 95th percentile precipitation, and CDD) at The Pas for the calibration period.

LARS-WG generally producing the smallest bias range for all the stations. SDSM using NCEP predictors produced a bias range of –18.39 mm to +18.18 mm while SDSM using CGCM3 predictors gave a slightly smaller bias range of –9.59 mm to +11.59 mm. Overall, LARS-WG had the best agreement with observed values.

- For the five day total rainfall, the results at The Pas generally show that the downscaled model results are closer to the observed data than the raw CGCM3 data, with all models generally having negative bias. LARS-WG generally has a

smaller bias than SDSM using NCEP and CGCM3 predictors, and SDSM using NCEP predictors generally had a smaller bias than SDSM using CGCM3 predictors. Overall, LARS-WG produced the best overall results, with a bias between –6.6 mm and +3.4 mm for all stations.

- For CCD, the results at The Pas show that generally the downscaled model results are closer to the observed values than the raw CGCM3 values, with all models generally having a negative bias. LARS-WG generally had a smaller bias than SDSM using NCEP and CGCM3 predictors. SDSM using CGCM3 predictors generally has a smaller bias than SDSM using NCEP predictors. While SDSM-CGCM3 produced a generally smaller bias for The Pas, LARS-WG again produced the best results for the remaining five stations, with a bias less than –3.39 days and +3.30 days for all stations, while SDSM using both NCEP and CGCM3 predictors had a bias range of –5.47 days to +2.13 days and –5.83 days to +1.23 days, respectively.

6.3.1.2 Temperature

Probability density functions (PDFs) are used to compare CGCM3 and the two downscaling models (LARS-WG and SDSM) with the observed statistical distribution of Tmax and Tmin. The results are shown in Figure 6.10 for The Pas. These PDFs demonstrate the problems associated with the distribution of raw temperature data from CGCM3, especially in simulating variability and extreme at all stations. These plots also illustrate how well the downscaled data reproduce the statistical distribution of the

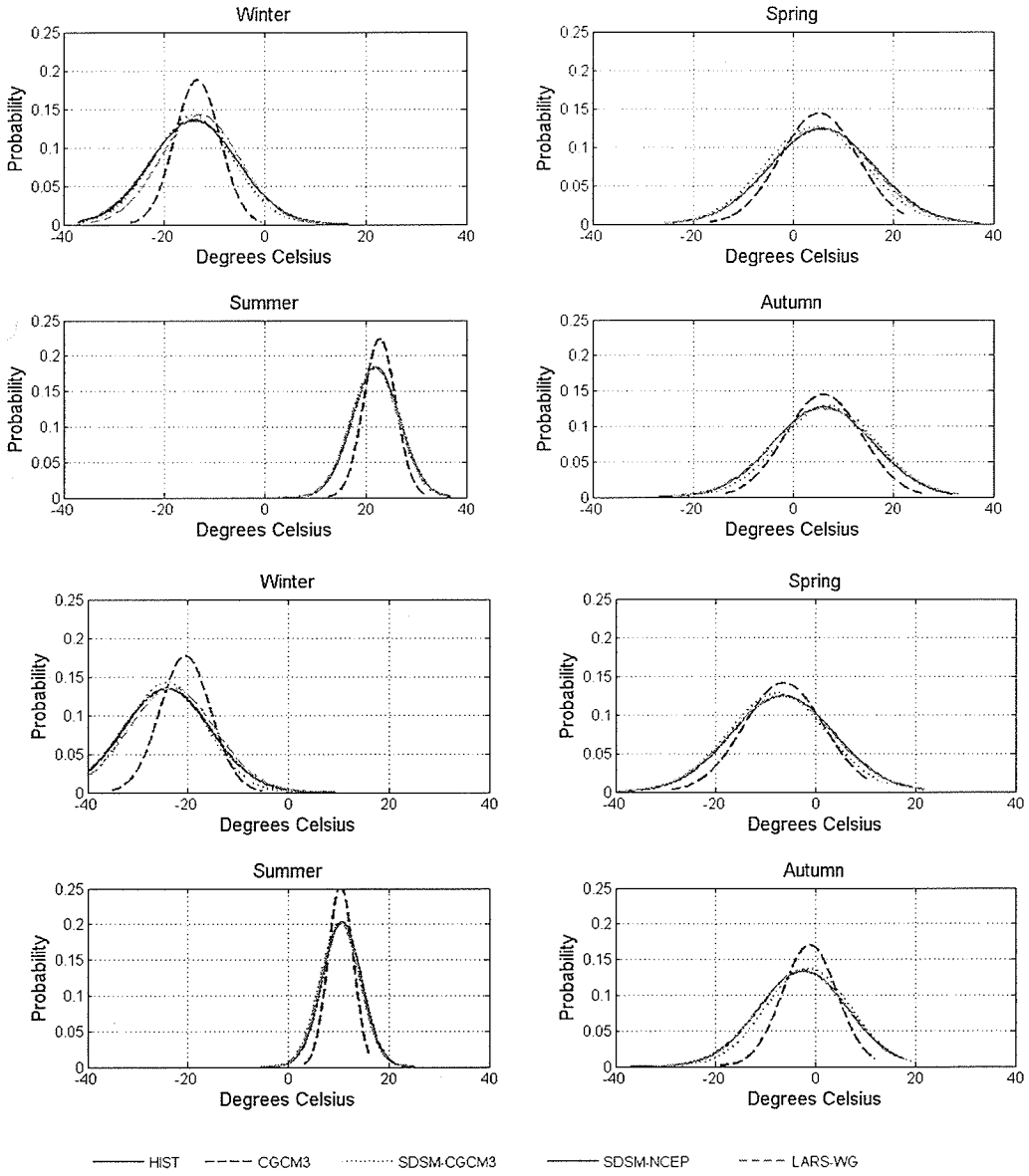

Figure 6.10: Probability density functions at The Pas for Tmax (top) and Tmin (bottom)

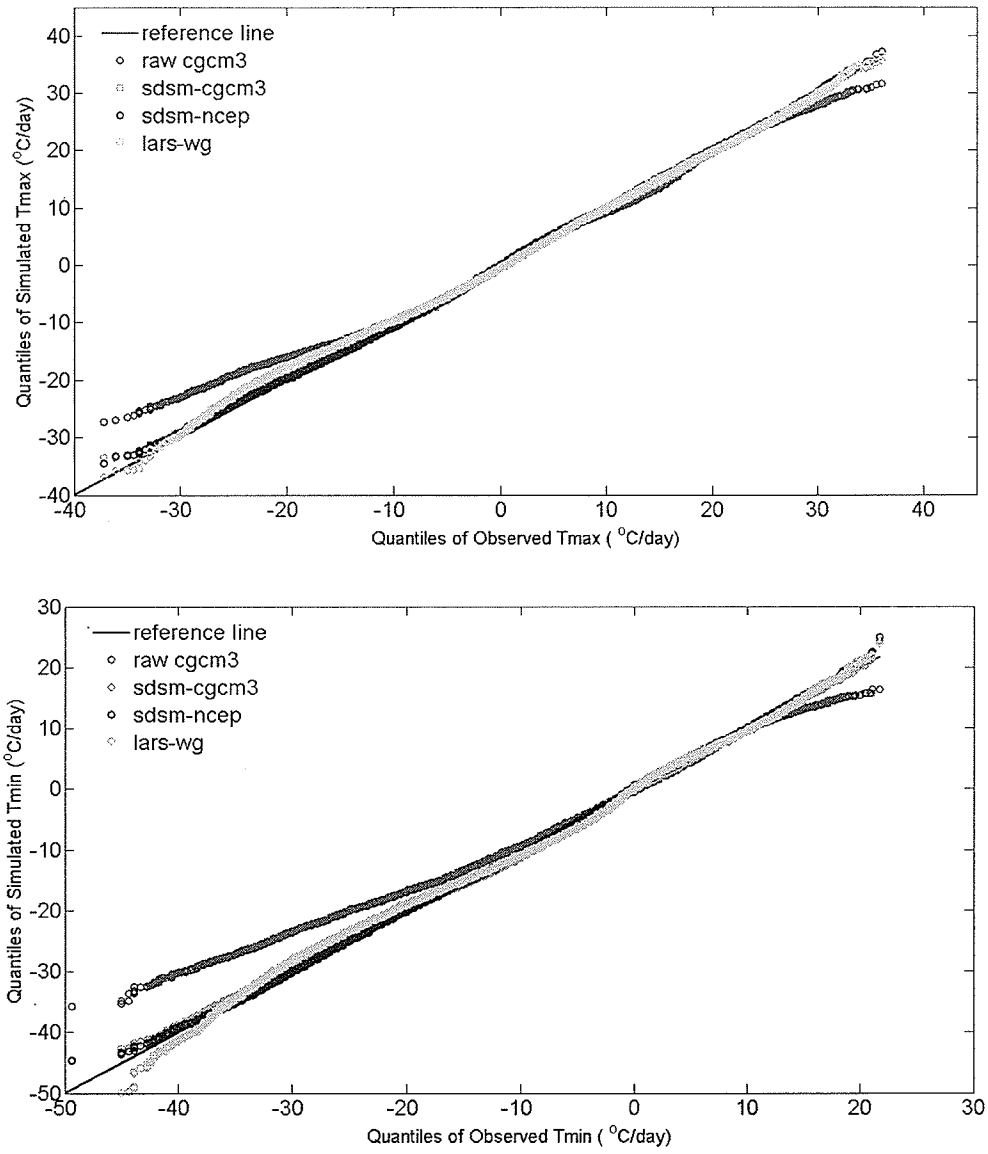

Figure 6.11: Quantile–quantile plots for Tmin and Tmax at The Pas (1961–1990)

observed data including the extremes and confirm that the downscaled data have improved the simulated distribution of Tmax and Tmin when compared to CGCM3. The results show that downscaling has vastly improved the simulated distribution of Tmax

and Tmin. Similar results were obtained for the remaining five climate stations. Generally, simulations are better with NCEP predictors than with CGCM3 predictors.

The quantile–quantile (Q-Q) plot for Tmax and Tmin at The Pas obtained with CGCM3, SDSM-NCEP, SDSM-CGCM3, and LARS-WG are shown in Figure 6.11. Generally, CGCM3 is overestimating the lower extreme values and under-estimating the upper extreme values. The downscaled models vastly improve the frequency distribution over CGCM3 by reducing the over- and underestimation of the lower quantiles of Tmin and Tmax. Results were very similar for the remaining five stations (not shown).

Seasonal box plots of the daily Tmin and Tmax at the Winnipeg, Brandon, Kenora, Sioux Lookout, Thompson, and The Pas stations were prepared to compare the seasonal mean values with the observed and simulated results over the calibration and validation periods. Generally, the downscaling results for daily Tmin and Tmax at each of the six stations reproduce the observed values well. The Pas station is presented in Figure 6.6 as representative box plots of the seasonal mean values of temperature. These plots show that the performance of LARS-WG, SDSM using NCEP predictors (SDSM-NCEP) and SDSM using CGCM3 predictors (SDSM-CGCM3) were generally in better agreement with the observed values both for the median and the IQR values than the CGCM3. The downscaled information appears to be an improvement over CGCM3 in all seasons and for all stations. The underestimation of the IQR and the maximum and minimum extremes (extremes) of the Tmin and Tmax distribution range are significantly reduced by downscaling, and the over- and underestimations of the median values are

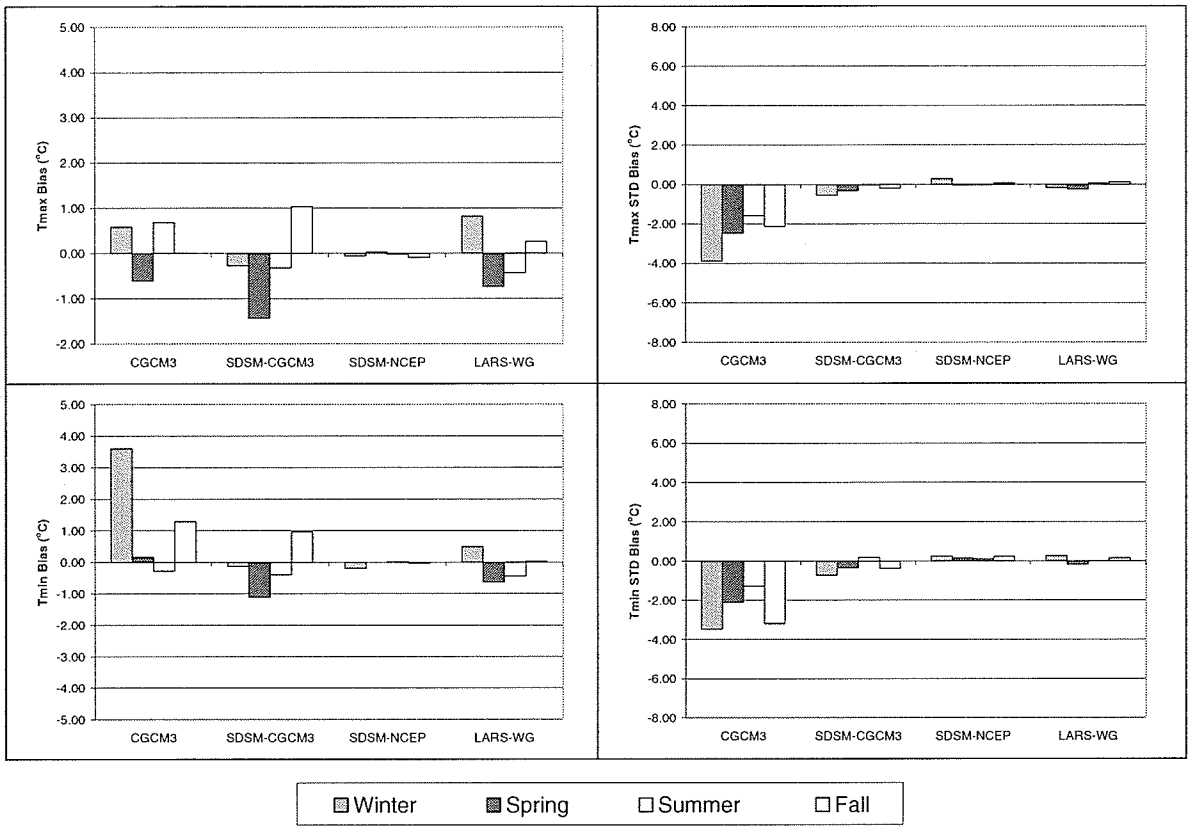

Figure 6.12: Seasonal biases of Tmin and Tmax at The Pas (1961–1990).

also reduced. Generally, LARS-WG and SDSM-CGCM3 tend to overestimate the median, Tmin and Tmax in the spring season and underestimate them in the autumn seasons. Overall, SDSM-NCEP has a better ability to reproduce the IQR, the extremes of the Tmin and Tmax distribution range, and the median values for all stations in all seasons than SDSM-CGCM3 and LARS-WG. Similar results were obtained on a monthly scale (not shown).

Bar plots of biases in the seasonal mean and standard deviation of Tmax and Tmin associated with both CGCM3 and the downscaled models at each of the six climate

stations have been plotted. Since the results for the stations are very similar, a bar plot of a representative sample (The Pas) is presented in Figure 6.12. This figure demonstrates that Tmin and Tmax data simulated by raw CGCM3 have strong biases (in terms of seasonal mean and standard deviation) for most of the seasons. CGCM3 data shows a warm mean bias for the winter and summer season while the rest of the seasons have a cold mean bias, similar to the results suggested by the seasonal PDFs. For the winter and summer seasons, the mean seasonal temperature bias for CGCM3 is higher than those corresponding to the downscaled models. The downscaled data from SDSM using CGCM3 predictors contain negative biases in the spring season and positive biases in the autumn season. The bias of SDSM-CGCM3 is larger than SDSM-NCEP. SDSM-NCEP did not show any large bias in any season, while LARS-WG showed a negative bias during the spring and summer season and a positive bias in the winter season. The seasonal bias in standard deviation between the observed and simulated values shown in Figure 6.12 suggest that the CGCM3 systemically underestimates the temperature variability for all seasons, while the downscaled models show considerably less bias with minor over- and underestimation of the variability. As noted in the PDF curves, Figure 6.12 also shows that SDSM-CGCM3 reduces the temperature biases compared to the raw CGCM3, in terms of both seasonal mean and standard deviation values. In general, while the downscaling performed with the NCEP predictors gives the best agreement with the observed data in terms of mean seasonal temperature and their standard deviations,

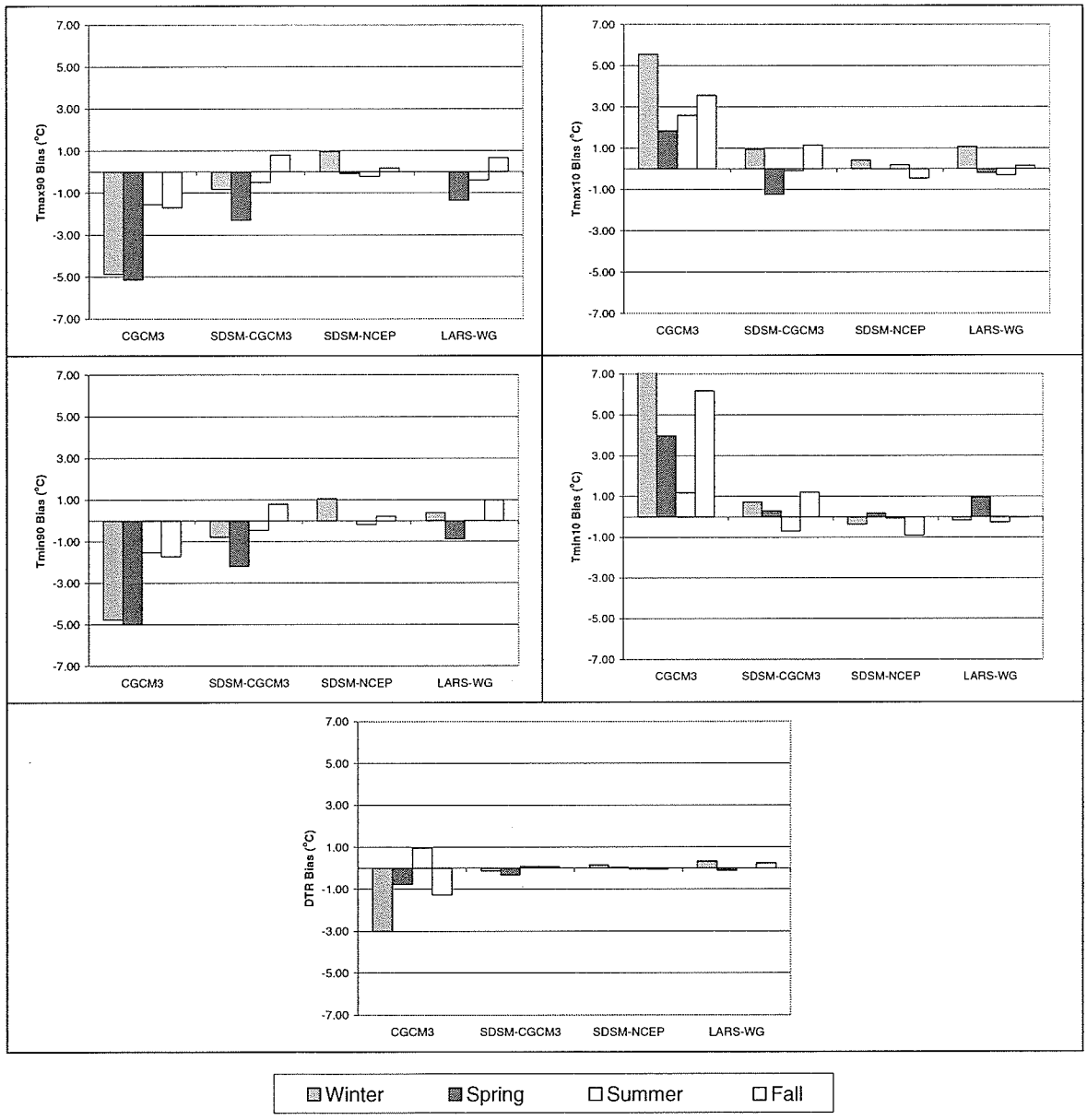

Figure 6.13: Seasonal biases of temperature indices (Tmax10, Tmax90, Tmin10, Tmin90 and DTR) at The Pas (1961–1990).

the downscaling from LARS-WG also gave very good results. Similar results were obtained on a monthly scale (not shown).

Over all the six climate stations, CGCM3's seasonal temperature biases range between −4.2°C and +4.5°C (with the highest biases being in spring season at Brandon and the lowest bias being in the summer season at Kenora) while that of downscaled models biases are smaller in the order of −2.0°C and +1.5°C suggesting a more systematic problem with the surface processes representation in the CGCM3 model compared to the downscaled models (Figure 6.6).

Seasonal bar plots are also used to compare the raw CGCM3 and downscaled temperature indices for the diurnal temperature range (DTR), the 10^{th} and 90^{th} percentile of Tmax (Tmax10 and Tmax90) and the 10^{th} and 90^{th} percentile of Tmin (Tmin10 and Tmin90) with the observed statistical distribution. These seasonal indices are shown in Figure 6.13 for The Pas with observed values as well as raw CGCM3, and SDSM-NCEP, SDSM-CGCM3, and LARS-WG. The plots show that generally the downscaled model results are closer to the observed values than the CGCM3:

- For the DTR indices, CGCM3 generally shows a negative bias while the two downscaling models generally show a moderate positive and negative bias for this index. The other five stations yield similar results for the DTR with LARS-WG generally showing the smallest bias range (−0.15°C to +0.41°C). SDSM using NCEP predictors had a bias range of −0.46°C to +0.40°C while SDSM

using CGCM3 predictors had a slightly larger bias range of −0.48°C to +0.59°C. Overall, both downscaling models have similar results.

- For the Tmin10 and Tmin90 results, CGCM3 generally has a negative bias for Tmin90 and a positive bias for Tmin10, while the downscaled model results all generally have a closer relationship to the observed data than CGCM3 plots at The Pas. SDSM-NCEP generally has the smallest bias for Tmin10 followed by LARS-WG and then SDSM-CGCM3. For the remaining five stations, the results were similar with LARS-WG yielding the smallest overall bias for Tmin10 and SDSM-NCEP yielding the smallest overall bias for Tmin 90.
- For the Tmax10 and Tmax90, CGCM3 tends to have a negative bias for Tmax90 and a positive bias for Tmax10 at The Pas. SDSM-CGCM3 tends to underestimate Tmax10 and Tmax90 for the spring season and overestimate the autumn season, while SDSM-NCEP generally has the smallest bias of the two downscaling models, with LARS-WG having slightly higher bias than SDSM-CGCM3. Similar results were obtained with the other five stations for Tmax10 and Tmax 90. LARS-WG generally has the smallest bias for Tmax10 and Tmax90 followed by SDSM-NCEP and then SDSM-CGCM3.

6.3.2 Validation Period (1991-2000)

Over the validation period (1991-2000), Tmax, Tmin, and precipitation values downscaled from SDSM and LARS-WG were analyzed for their basic distribution, mean, median values, and variability. Generally, the downscaling results for Tmin and Tmax at

Table 6.3: Average of downscaled results for precipitation, Tmax, and Tmin for Winnipeg, Brandon, Kenora, Sioux Lookout, The Pas and Thompson for all four seasons during the calibration and validation periods. Where Q1 and Q3 represent the 25th and 75th percentile respectively.

	Calibration Period (1961-1990)			*Validation Period (1991-2000)*		
	SDSM-CGCM3	**SDSM-NCEP**	**LARS-WG**	**SDSM-CGCM3**	**SDSM-NCEP**	**LARS-WG**
	Precipitation bias (mm/day)			**Precipitation bias (mm/day)**		
Q1	−0.15	−0.08	+0.08	−0.23	−0.14	+0.06
Median	−0.02	+0.06	+0.10	−0.03	+0.04	+0.12
Q3	+0.10	+0.13	+0.12	+0.26	+0.10	+0.15
	Tmax bias (°C/season)			**Tmax bias (°C/season)**		
Q1	−0.70	−0.10	−0.49	−0.49	−0.59	−0.49
Median	−0.27	+0.01	−0.26	+0.19	−0.36	−0.22
Q3	+0.08	+0.04	+0.12	+1.54	+0.10	+0.22
	Tmin bias (°C/season)			**Tmin bias (°C/season)**		
Q1	−0.70	−0.07	−0.53	−0.12	−0.16	−0.49
Median	−0.32	+0.00	−0.13	+0.80	+0.17	−0.07
Q3	+0.14	+0.05	+0.36	+1.62	+0.35	+0.35

each of the six stations reproduced the observed values well over the calibration and validation periods. The Pas station is presented as representative sample with box plots of the seasonal mean values of Tmax and Tmin shown in Figure 6.6. These plots show that the performance of SDSM using NCEP and LARS-WG is very good and almost as good over the validation period as it is over the calibration period. Results obtained for the downscaled data at the other five stations (Winnipeg, Brandon, Kenora, Sioux Lookout and Thompson) were similar (not shown here). Generally, over the validation period SDSM using NCEP predictors and LARS-WG were able to reproduce the median characteristics of seasonal mean precipitation reasonably well as shown in Figure 6.6 for The Pas. SDSM using CGCM3 predictors has difficulty reproducing the seasonal mean, the IQR, and the outliers.

The distribution of the seasonal median (50th quartile), 25th quartile (Q1), and 75th quartile (Q3), values averaged at all six stations over the validation and calibration periods are shown in Table 6.3. The seasonal mean values of the observed and simulated results for the calibration (1961–1990) and validation (1991–2000) periods were compared. With a few exceptions, the downscaling results for Tmax, Tmin, and precipitation values at each station reproduce the observed values reasonably well. For precipitation, the performance of LARS-WG and SDSM using NCEP predictors is very good and almost as good over the validation period as it is over the calibration period. While SDSM using the CGCM3 shows little change in the median values over the validation period, there is a noticeably increased bias in Q1 and Q3 over the validation period. For Tmin and Tmax, the performance of LARS-WG is also very good and almost as good over the validation period as it is over the calibration period. SDSM using NCEP predictors has slightly more bias over the validation period than the calibration period with an increased bias for the median values and the Q1 and Q3 values. SDSM using CGCM3 predictors does not perform as well as LARS-WG and SDSM-NCEP with considerably more bias in the validation period compared to the calibration period. For Tmax, the Q1 and Q3 values for SDSM-CGCM3 range from –0.70°C to +0.08°C (0.78°C range) for the calibration period and increased to –0.49°C to +1.54°C (2.03°C range) for the validation period.

6.3.3 Summary of Downscaling Results

In summary, it was found LARS-WG was able to produce daily precipitation statistics in closer agreement with those of the observed data, while SDSM provided extreme temperature statistics more accurate than the LARS-WG. The comparison between some selected statistics of observed climate data and those of climate data generated by the two models indicates that LARS-WG yields precipitation statistics that are more comparable to those of the observed data than the SDSM. In addition, SDSM-NCEP and SDSM-CGCM3 demonstrated weakness in simulating the precipitation extreme indices. Since confidence in future scenarios at a local scale to a large extent depends on the ability of the downscaled model to reproduce the observed climate regimes, it would be difficult to have great confidence in precipitation downscaled for future climate scenarios if the impact model required accurate representation of precipitation extremes. In the selection of predictors for precipitation in the SDSM process there was a relatively low explained variance which resulted in the inability of SDSM to capture the characteristics of the variability of precipitation.

With respect to temperature the comparison between some selected statistics of observed climate data and those of climate data generated by the two models indicates that SDSM and LARS-WG were able to describe adequately the observed statistics of daily temperature extremes, and SDSM was found to be somewhat more accurate than LARS-WG.

In many instances, SDSM with CGCM3 predictors degraded the performances of SDSM. This was due to a bias present in the predictor variables which propagated into the downscaling model. Ideally, various GCM model predictors should be tested with SDSM to determine if this was just a strong bias present in CGCM3 predictors or a weakness of the downscaling model itself.

6.4 Climate Change Scenarios

SDSM and LARS-WG were used to simulate climate change scenarios for two future time periods (2050s and 2090s) with SRESA1B, SRESA2, and SRESB1. Figures 6.14 to 6.15 illustrate the results by presenting the simulated increase or decrease in variables between the current (1961-1990) and the future 2050s and 2090s time periods for each of the downscaling methods.

The results show that both SDSM and LARS-WG project an increase in the mean temperature values at all stations with the 2090s displaying slightly larger increases than the 2050s. LARS-WG and CGCM3 project temperatures increase between +2.5°C to +4.5°C for all stations with all SRES while SDSM projects slightly higher temperature increases between +2.5°C to +7.5°C. Generally simulations for LARS-WG and CGCM3 are within 0.2°C of each other with LARS-WG projecting the higher temperature increase of the two. The lowest temperature increases were simulated for the SRESB1 scenario, while the highest temperature increases are simulated for the SRESA2 scenario. The SRESA1B scenario simulations were generally higher than SRESB1 and lower than SRESA2.

In general, all models project an increase in precipitation for the 2050s and 2090s at all stations. LARS-WG projections for future precipitation regimes are generally larger than SDSM for the 2050s and somewhat mimics CGCM3, due to the nature of how the model develops future scenarios. There are a few exceptions where SRESA2 simulations from SDSM are higher than LARS-WG at some stations especially for the 2090s. SRESB1 projections of precipitation are the highest with SRESA2 being the lowest. The lowest precipitation increases were simulated for the SRESB1 scenario, while the highest precipitation increases are simulated for the SRESA2 scenario. The SRESA1B scenario simulations were generally higher than SRESB1 and lower than SRESA2.

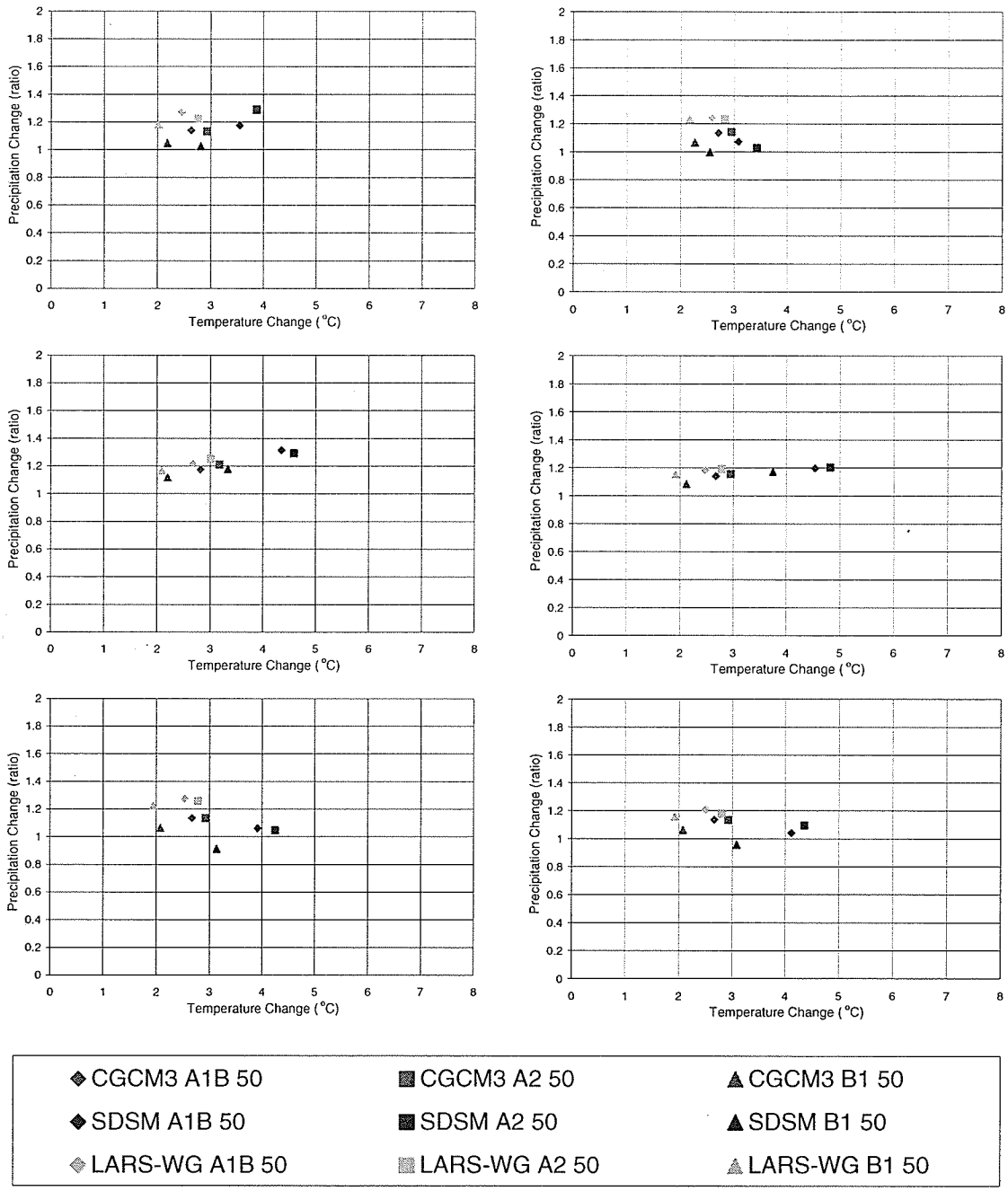

Figure 6.14: Climate change scenarios (2050s) - 1st Row (L): Winnipeg (R): Brandon, Middle Row (L): Thompson (R): The Pas, Bottom Row (L): Kenora (R): Sioux Lookout

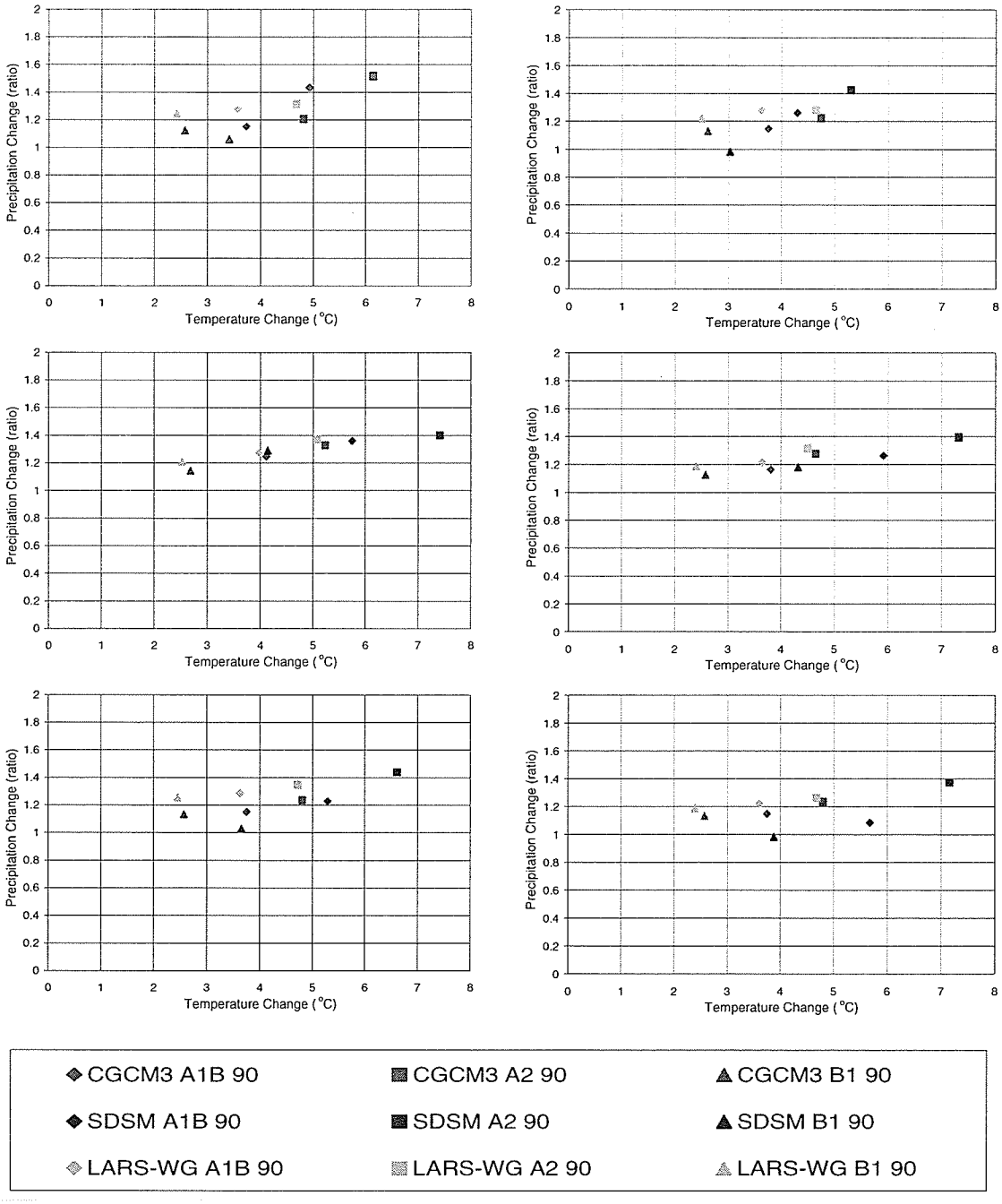

Figure 6.15: Climate Change Scenarios (2090s) - 1st Row (L): Winnipeg (R): Brandon, Middle Row (L): Thompson (R): The Pas, Bottom Row (L): Kenora (R): Sioux Lookout

Chapter 7

Conclusions

Historical trend analysis and future climate change studies have shown that past and future temperatures in central Canada (and around the world) are and will continue to rise. It is anticipated that these temperature changes will impact the world's resources, through an increase in precipitation and evaporation. Therefore, resource managers must have a comprehensive understanding of the scope, magnitude, and timing of these potential impacts to address future climate change.

Global climate models (GCMs) are used to project future climate change. However, due to their coarse spatial scale they have fundamental weaknesses at sub-grid scales, which is a critical limitation for direct use in many impact models. This study has shown that CGCM3 exhibits strong biases in terms of means and standard deviation for both temperature and precipitation at local sites. In order to overcome these weaknesses, downscaling techniques have been developed. Confidence in future climate change scenarios at a local scale depends to a large extent on how these downscaling models can re-construct the observed climate.

In this study, two popular statistical downscaling techniques (LARS-WG and SDSM) were evaluated for simulating precipitation and temperature series for six stations

in the central Canada. The evaluation of these models consisted of examining their ability to simulate means and extreme indices.

The evaluation between selected statistics of observed climate data and those of climate data generated by the two models indicates that LARS-WG can reproduce the daily precipitation statistics of the observed data better than SDSM. However, both models were unable to accurately reproduce all the observed statistics of precipitation. SDSM and LARS-WG were both able to describe the observed statistics of daily mean and extreme temperature, with SDSM-NCEP generally more accurate than LARS-WG. The downscaling process in both cases improved the CGCM3 output by reducing the biases found in the raw CGCM3 and improving the variability. Therefore, the added value from the downscaled results confirms that downscaling methods are preferred to using the raw CGCM3 outputs.

During the selection of predictor variables in the SDSM process, it was determined that there was a relatively low explained variance for precipitation. This is due to precipitation's stochastic nature and indicates a potential limitation for downscaling precipitation with this model. There was also a bias present in the predictor variables from CGCM3 which propagated into the SDSM process. This was noted when SDSM's skill was degraded using CGCM3 predictors. Future studies must test a suite of predictor variables from other GCMs to determine if this is a fundamental weakness of SDSM or just a limitation from using predictors from CGCM3. Regional climate model (RCM) predictors could also be tested to determine if they improve the performance of

this model, since precipitation needs mesoscale forcing and feedbacks that are better resolved in RCMs.

Climate change scenarios from both downscaling models indicated that temperatures for the future will continue to increase. Generally, precipitation is projected to increase in the future as well. A climate change scenario from LARS-WG relies heavily on outputs from the GCM to develop the scenario file. However, these surface variables are not well simulated by the GCM, therefore the reliability of future simulations will only be as reliable as the GCM used. SDSM relies heavily on the selection of predictor variables which will dominate in the future. If these predictors do not capture accurately the climate change signal, the future projections will likely not be accurate. Both models therefore demonstrate weakness for future projections.

Future studies are required to understand the influence of predictor variables for this study region. Even though the selection of predictors was based on theories from other studies that determined which processes will dominate in the future, these theories must be confirmed for this region. RCM data should also be tested to develop the scenario file in LARS-WG. The performance of these two models must be evaluated using data from additional GCMs or RCMs to assess the reliability of generated future climate scenarios at local sites. In addition it is recommended that one compare the performance of SDSM and LARS-WG using data from other sites with different climatic conditions

In general, this study presented one method of evaluating the added value of

downscaling using both means and some extreme indices. It also presented future climate change scenarios derived from these downscaling models. In order to understand how these climate change scenarios can be used in impact models, future studies are recommended to include an applied element (i.e. hydrological impacts). This should consider how the results might allow resource managers to make more informed decisions on resource management to adapt to future climate uncertainty.

In terms of practical application, calibration of LARS-WG is much simpler than SDSM, since the calibration of SDSM is based on a complex procedure in order to be able to successfully establish the relationships between large-scale predictor variable and the surface weather variables at a local site.

Bibliography

Allen, R. G., Smith, M., Raes, D., and Perreira, L. S. (1998). "Crop evapotranspiration: Guidelines for computing crop water requirements." FAO Irrigation and Drainage Paper 56.

Appiah-Adjei, E. K. (2006). "Climate Change Impacts on Groundwater Recharge in Gulf Islands, Canada," MSc. Thesis, Lund University, Lund, Sweden.

Baede, A. P. M., Ahlonsou, E., Ding, Y., Schimel, D., Bolin, B., and Pollonais, S. (2001). "Climate Change 2001: The Scientific Basis, Contribution from Working Group I to the Third Assessment Report of the Intergovernmental Panel on Climate Change." The Climate System: an Overview, J. T. Houghton, Y. Ding, D. J. Griggs, M. Noguer, P. J. van der Linden, K. Dai, K. Maskell, and C. A. Johnson, eds., Cambridge University Press, Cambridge, United Kingdom.

Barrow, E., and Lee, R. J. (2000). "Climate Change and Environmental Assessment Part 2: Climate Change Guidance for Environmental Assessments." Canadian Environmental Assessment Agency, Victoria, B.C.

Bristow, K. L., and Campbell, G. S., 1984 (1984). "On the relationship between incoming solar radiation and daily maximum and minimum temperature." *Agricultural and Forest Meteorology* 31, 159-166.

Carter, T. R., Alfsen, K., Barrow, E., Bass, B., Dai, X., Desanker, S. R., Gaffin, F., Giorgi, M., Hulme, M., Lal, M., Mata, L. J., Mearns, L. O., Mitchell, J. F. B., Morita, T., Moss, R., Murdiyarso, J. D., Pabon-Caicedo, J. D., Palutikof, J., Parry, M. L., Rosenzweig, C., Seguin, B., Scholes, R. J., and Whetton, P. H. (2007). "General Guidelines on the use of Scenario Data for Climate Impact and Adaptation Assessment." Finnish Environmental Institute, Helsinki, Finland.

Choux, M. (2005). "Development of New Predictors Climate Variables For Statistical Downscaling of Daily Precipitation Process," MSc. Thesis, McGill University, Montreal, Quebec.

Cubasch, U., Meehl, G. A., Boer, G. J., Stouffer, R. J., Dix, M., Noda, A., Senior, C. A., Raper, S., and Yap, K. S. (2001). "Projections of Future Climate Change." Climate Change 2001: The Scientific Basis, J. T. Houghton, Y. Ding, D. J. Griggs, M. Noguer, P. J. van der Linden, K. Dai, K. Maskell, and C. A. Johnson, eds., Cambridge University Press, Cambridge, United Kingdom.

Dibike, Y. B., and Coulibaly, P. (2007). "Validation of hydrologic models for climate scenario simulation: The case of Saguenay watershed in Québec." *Hydrological Processes*, 21(23), 3123-3235.

Dibike, Y. B., Gachon, P., St-Hilaire, A., Ouarda, T. B. M. J., and Nguyen, V.-T.-V. (2007). "Uncertainty analysis of statistically downscaled temperature and precipitation regimes in northern Canada." *Theoretical and Applied Climatology*, In press.

Donatelli, M., and Campbell, G. (1998). "A model to estimate global solar radiation using daily air temperature." Proceedings of the 5th ESA Congress, Nitra, Slovak Republic.

Gachon, P. (2007). "Temperature change signals in northern Canada." *International Journal of Climatology*, in press.

Gachon, P., Radojevic, M., Harding, A., and Parishkura, D. (2008). "Predictor Datasets Derived from the CGCM3.1 T47and NCEP/NCAR Renalysis." Data Access Integration, Montreal.

Gachon, P., St-Hilaire, A., Ouarda, T., Nguyen, V. T. V., Lin, C., Milton, J., Chaumont, D., Goldstein, J., Hessami, M., Nguyen, T. D., Selva, F., Nadeau, M., Roy, P., Parishkura, D., Major, N., Choux, M., and Bourque, A. (2005). "A First Evaluation of the Strength and Weaknesses of Statistical Downscaling Methods for Simulating Extremes Over Various Regions in Eastern Canada." Climate Change Action Fund, Montreal, Quebec.

Giorgi, F., and Mearns, L. O. (1999). "Regional climate modeling revisited: An introduction to the special issue." *J. Geophys. Res.*, 104, 6335-6352.

Girogi, F., Hewitson, B. C., Christensen, J. H., Hulme, M., Von Storch, H., Whetton, P., Jones, R. G., Mearns, L. O., and Fu, C. (2001). "Regional Climate Information-Evaluation and Projections." Climate Change 2001: The Scientific Basis, J. T. Houghton, Y. Ding, D. J. Griggs, M. Noguer, P. J. van der Linden, K. Dai, K. Maskell, and C. A. Johnson, eds., Cambridge University Press, Cambridge, United Kingdom.

Hassan, H., Aramaki, T., Hanaki, K., Matsuo, T., and Wilby, R. L. (1998). "Lake stratification and temperature profiles simulated using downscaled GCM output." *Journal of Water Science and Technology*, 38, 217–226.

Haylock, M. R., Cawley, G. C., Harpham, C., Wilby, R. L., and Goodess, C. (2006). "Downscaling heavy precipitation over the UK: A comparison of dynamical and statistical methods and their future scenarios." *International Journal of Climatology*, 26(10), 1397-1415.

Hessami, M., Gachon, P., Taha, B. M. J. O., and St, H. (2008). "Automated regression-based statistical downscaling tool." *Environmental Modelling and Software*, 23(6), 813-834.

Hewitson, B. C. (1999). "Deriving regional precipitation scenarios from General Circulation Models." South African Water Research Commission.

Hewitson, B. C., and Crane, R. G. (1996). "Climate downscaling: Techniques and applications." *Climate Research*, 7(2), 85-95.

Hostetler, S. W. (2005). "Hydrologic and atmospheric models: The (continuing) problem of discordant scales." *Climatic Change*, 27(4), 345-350.

Houghton, J. T., Callander, B. A., and Varney, S. K. (1992). "Climate Change 1992: The IPCC Supplementary Report." Cambridge University Press.

Huth, R. (1999). "Statistical downscaling in Central Europe: Evaluation of methods and potential predictors." *Climate Research*, 13(91-101).

IPCC-TGCIA. (1999). "Guidelines on the Use of Scenario Data for Climate Impact and Adaptation Assessment." Intergovernmental Panel on Climate Change.

IPCC. (2000). *Special Report on Emissions Scenarios, A Special Report of Working Group III of the Intergovernmental Panel on Climate Change*, Cabmbridge University Press, New York.

IPCC. (2001). *Climate Change 2001: The Scientific Basis. Contribution of the Working Group I to the Third Assessment Report of the Intergovernmental Panel on Climate Change*, Cambridge University Press, Cambridge, United Kingdom.

IPCC. (2007). "Climate Change 2007: The Physical Science Basis. Contribution of Working Group I to the Fourth Assessment Report of the Intergovernmental Panel on Climate Change." Summary for Policymakers, S. Solomon, D. Qin, M. Manning, Z. Chen, M. Marquis, K. B. Averyt, M. Tignor, and H. L. Millers, eds., Cambridge University Press, Cambridge, United Kingdom.

Jones, R. G., Murphy, J. M., and Noguer, M. (1995). "Simulation of Climate Change over Europe using a nested regional model. Part I: Assessment of control climate including sensitivity to location of lateral boundaries." *Quarterly Journal of the Royal Meteorological Society.*, 121(526), 1413-1449.

Källén, E., Kattsov, V., Walsh, J., and Weatherhead, E. (2001). "Report from the Arctic Climate Impact Assessment Modelling and Scenario Workshop." Arctic Climate Impact Assessment Modelling and Scenarios Workshop, ACIA Secretariate, Fairbanks, Stockholm, Sweden.

Kalnay, E., Kanamitsu, R., Kistler, R., Collins, W., Deaven, L., Gandin, M., Iredell, S., Saha, G., White, J., Woollen, Y., Zhu, M., Chelliah, M., Ebisuzaki, W., Higgins, W., Janowiak, K., Mo, C., Ropelewski, J., Wang, A., Leetmaa, R., Reynolds, R.,

Jenne, R., and Joseph, D. (1996). "The NCEP/NCAR 40-year reanalysis project." *Bulletin of American Meteorological Society*, 77, 437-471.

Le Treut, H., Somerville, R., Cubasch, U., Ding, Y., Mauritzen, C., Mokssit, A., Peterson, T., and Prather, M. (2007). "Historical Overview of Climate Change Science " Climate Change 2007: The Physical Science Basis. Contribution on Working Group I to the Fourth Assessment Report of the Intergovernmental Panel on Climate Change, S. Solomon, D. Qin, M. Manning, Z. Chen, M. Marquis, K. B. Averyt, M. Tignor, and H. L. Millers, eds., Cambridge University Press, Cambridge, United Kingdom.

Lines, G. S., and Pancura, M. (2004). "Application of downscaling techniques for assessing climate change variability and extremes in Atlantic Canada." *Geophysical Research Abstracts.*

Loaiciga, H. A., Valdes, J. B., Vogel, R., Garvey, J., and Schwarz, H. (1996). "Global warming and the hydrologic cycles." *Journal of Hydrology*, 174, 83-127.

McAvaney, B. J., Covey, C., Joussaume, S., Kattsov, V., Kitoh, A., Ogana, W., Pitman, A. J., Weaver, A. J., Wood, R. A., and Zhao, Z.-C. (2001). "Model Evaluation." Climate Change 2001: The Scientific Basis, J. T. Houghton, Y. Ding, D. J. Griggs, M. Noguer, P. J. van der Linden, K. Dai, K. Maskell, and C. A. Johnson, eds., Cambridge University Press, Cambridge, United Kingdom.

Mearns, L. O., Giorgi, F., Whetton, P. H., Pabon, D., Hulme, M., and Lal, M. (2003). "Guidelines for Use of Climate Scenarios Developed from Regional Climate Model Experiments." Data Distribution Center of the Intergovernmental Panel on Climate Change.

Mearns, L. O., Hulme, M., Carter, T. R., Leemans, R., Lal, M., Whetton, P., Hay, L., Jones, R. N., Katz, R., Kittel, T., Smith, R., and Wilby, R. L. (2001). "Climate Scenario Development." Climate Change 2001: The Scientific Basis, J. T. Houghton, Y. Ding, D. J. Griggs, M. Noguer, P. J. van der Linden, K. Dai, K. Maskell, and C. A. Johnson, eds., Cambridge University Press, Cambridge, United Kingdom.

Mekis, É., and Hogg, W. D. (1999). "Rehabilitation and analysis of Canadian daily precipitation time series." *Atmosphere-Ocean*, 37(1), 53-85.

Mekis, E., and Vincent, L. (2005). "Precipitation and temperature related indices for Canada." 85th American Meteorological Society Annual Meeting, San Deigo, California.

Mohammad, S. K., Coulibaly, P., and Dibike, Y. (2006). "Uncertainty analysis of statistical downscaling methods using Canadian Global Climate Model predictors." *Hydrological Processes*, 20(14), 3085-3104.

Murphy, J. (1998). "An evaluation of Statistical and Dynamical Techniques for Downscaling Local Climate." *Journal of Climate*, 12, 2256-2284.

Nelson, R. (2007). "ClimGen- Climatic Data Generator User's Manual." Washington University.

Nguyen, V. T. V., Nguyen, T. D., and Gachon, P. (2006). "On the linkage of large-scale climate variability with local characteristics of daily precipitation and temperature extremes: An evaluation of statistical downscaling methods." *Advances in Geosciences*, 4(16), 1-9.

Rascko, P., Sziedlo, L., and Semenov, M. (1991). "A serial approach to local stocastic weather models." *Ecological Modelling*, 57(27-41).

Richardson, C. W. (1981). "Stochastic simulation of daily precipitation, temperature, and solar radiation." *Water Resources Research*, 17, 182-190.

Saelthun, N. R., and Bark, L. J. (2003). "Climate Change Scenarios for the SCANNET Region." The Norwegian Institute for Water Research.

Schubert, S. (1998). "Downscaling local extreme temperature changes in south-eastern Australia from CSIRO Mark2 GCM." *International Journal of Climatology*, 18, 1419-1438.

Semenov, M., and Barrow, E. (1997). "Use of a stochastic weather generator in the development of climate change scenarios." *Climatic Change*, 35, 297-414.

Semenov, M., and Barrow, E. (2002). "A Stochastic Weather Generator for Use in Climate Impact Studies." Hertfordshire, UK, Rothamsted Research.

Semenov, M., Brooks, R. J., Barrow, E. M., and Richardson, C. W. (1998). "Comparison of WGEN and LARS-WG stochastic weather generators in diverse climates." *Climate Research*, 10, 95-107.

Smith, J. B., and Hulme, M. (1998). "Climate change scenarios." UNEP Handbook on Methods for Climate Change Impact Assessment and Adaptation Studies I. Burton, J. F. Feenstra, J. B. Smith, and R. S. J. Tol, eds., Vrije Universiteit, Amsterdam.

USEPA. (2006). "Data Quality Assessment: Statistical Methods for Practitioners EPA QA/G-9S." Office of Environmental Information, Washington, D.C.

Vincent, L. A., Zhang, X., Bonsal, B. R., and Hogg, W. D. (2002). "Homogenization of daily temperatures over Canada." *Journal of Climate*, 15, 1322-1334.

von Storch, H., Zorita, E., and Cubasch, U. (1993). "Downscaling of global climate change estimates to regional scales: An application to Iberian rainfall in wintertime." *Journal of Climate*, 6, 1161-1171.

Wigley, R. W. L., Jones, P. D., Briffa, K. R., and Smith, G. (1990). "Obtaining sub-grid scale information from coarse resolution general circulation model outputs." *Journal of Geophysical Reearch* 94, 1943-1953.

Wilby, R. L., Charles, S. P., Zorita, E., Timbal, B., Whetton, P., and Mearns, L. P. (2004). "Guidelines for use of climate scenarios developed from statistical downscaling methods." Data Distribution Center of the International Panel on Climate Change.

Wilby, R. L., and Dawson, C. (2004). "Using SDSM Version 3.1- A decision support tool for the assessment of regional climate change impacts." SDSM User Manual.

Wilby, R. L., Dawson, C. W., and Barrow, E. M. (2002). "SDSM- a decision support tool for the assessment of regional climate change impacts." *Environmental Modelling and Software*, 17, 147-159.

Wilby, R. L., Hay, L. E., Gutowski, W. J., Arritt, J., R.W., Takle, E. S., Leavesley, G. H., and Clark, M. (2000). "Hydrological responses to dynamically and statistically downscaled general circulation model output." *Geophysical Research Letters*, 27, 1199-1202.

Wilby, R. L., Hay, L. E., and Leavesley, G. H. (1999). "A comparison of downscaled and raw GCM output: Implications for climate change scenarios in the San Juan River Basin, Colorado. ." *Journal of Hydrology*, 225(67-91).

Wilby, R. L., and Wigley, T. M. L. (2000). "Precipitation predictors for downscaling: Observed and general circulation model relationships." *International Journal of Climatology*, 20(6), 641-661.

Wilby, R. L., Wigley, T. M. L., Conway, D., Jones, P. D., Hewitson, B. C., Main, J., and Wilks, D. S. (1998). "Statistical downscaling of general circulation model output: a comparison of methods." *Water Resources Research*, 34, 2995-3008.

Wilks, D. S., and Wilby, R. L. (1999). "The weather generator game: A review of stochastic weather models." *Progress in Physical Geography*, 23(3), 329-358.

Xu, C. (1999). "Climate change and hydrologic models: a review of existing gaps and recent research." *Water Resources Management*, 13(5), 369-382.

Zhang, X., L. , Vincent, W. D., and Hogg, A. (2000). "Temperature and precipitation trends in Canada during the 20th Century." *Atmosphere-Ocean*, 38(3), 395-429.

Appendix A

Airflow Indices

The airflow predictor variables (wind, divergence and vorticity) are derived at the standard pressure levels from the CGCM3 raw data as follows (Gachon et al. 2008):

- The geostrophic wind (zonal (u) and meridonal (v) components) are derived from the pressure gradients and are computed by the following equations:

$$u_g = \frac{1}{2\Omega R}\frac{1}{\sin\varphi}\frac{\partial \varphi}{\partial \varphi} \qquad \textbf{A.1}$$

$$v_g = \frac{1}{2\Omega R}\frac{1}{\sin\varphi\cos\varphi}\frac{\partial \varphi}{\partial \lambda} \qquad \textbf{A.2}$$

where $\varphi = \frac{1}{g}p$ is the geopotential height, R is the radius of the Earth, λ and φ are the longitude and latitude respectively and Ω is the angular speed of the Earth (7.27×10^{-5} s^{-1}).

- The divergence ($\overline{\nabla}$) term is calculated from the following equation:

$$\overline{\nabla} \bullet \vec{V}_g = -\frac{1}{2\Omega R^2}\left[\frac{1}{\sin\varphi\cos\varphi}\frac{\partial^2 \varphi}{\partial\lambda\partial\varphi} + \frac{1}{\cos^2\varphi}\frac{\partial\varphi}{\partial\lambda} - \frac{\partial}{\partial\varphi}\left(\frac{1}{\cos\phi\sin\varphi}\frac{\partial\varphi}{\partial\lambda}\right)\right] \qquad \textbf{A.3}$$

- The vorticity (ζ) is computed from the pressure gradients using the following equation:

$$\zeta_g = \frac{1}{2\Omega R^2}\left(\frac{1}{\sin\varphi}\frac{\partial^2\varphi}{\partial\lambda\partial\varphi}\right) + \frac{\partial}{\partial\varphi}\left(\frac{1}{\cos^2\varphi\sin\varphi}\frac{\partial\varphi}{\partial\lambda}\right) + \frac{1}{\cos\varphi}\frac{\partial\varphi}{\partial\varphi} \qquad \textbf{A.4}$$